Programme Area: Nuclear

Project: Natural Hazards Phase 3

Title: Case Study 1: Trawsfynydd

Abstract:

This document introduces the location and a demonstration of the hazard characterisation methodologies for:
• Extreme temperatures
• Seismic, geological and volcanic hazards including ash deposition
• Natural hazard combinations

Context:

The Natural Hazards Review project will develop a framework and best practice approach to characterise natural hazards and seek to improve methodologies where current approaches are inefficient. This is to improve energy system infrastructure design and the project is intended to share knowledge of natural hazards across sectors. The project will be completed in three stages. Phase one will focus on a gap analysis. Phase two will look at developing a series of improved methodologies from the gaps identified in phase one, and phase three will demonstrate how to apply these methodologies. Finally, phase 3 will develop a "how to" guide for use by project engineers.

Enabling Resilient UK Energy Infrastructure:
Natural Hazard Characterisation Technical Volumes
and Case Studies

Case Study 1:
Trawsfynydd

Legal Statement

Authors: Kate Brown, Erika Palin, Kate Salmon, Michael Sanderson, Emilie Vanvyve (Met Office); Dimitrios Kourepinis, Neil Lovett (Mott MacDonald)
Chief Technical Officer: Hugo Winter (EDF Energy)

Version	Date	Details
0.1	16/02/18	Submitted for IPR
0.2	08/03/18	IPR comments addressed and submitted to CTO
1.0	26/03/18	CTO comments addressed and submitted to ETI
2.0	06/06/18	ETI and Steering Committee comments addressed

This document forms part of the Energy Technologies Institute (ETI) project 'Low Carbon Electricity Generation Technologies: Review of Natural Hazards', funded by the ETI and led in delivery by the EDF Energy R&D UK Centre. The aim of the project has been to develop a consistent methodology for the characterisation of natural hazards, and to produce a high-quality peer-reviewed set of documents suitable for use across the energy industry to better understand the impact that natural hazards may have on new and existing infrastructure. This work is seen as vital given the drive to build new energy infrastructure and extend the life of current assets against the backdrop of increased exposure to a variety of natural hazards and the potential impact that climate change may have on the magnitude and frequency of these hazards.

The first edition of *Enabling Resilient UK Energy Infrastructure: Natural Hazard Characterisation Technical Volumes and Case Studies* has been funded by the ETI and authored by EDF Energy R&D UK Centre, with the Met Office and Mott MacDonald Limited. The ETI was active from 2007 to 2019, but to make the project outputs available to industry, organisations and individuals, the ETI has provided a licence to the Institution of Mechanical Engineers and Institution of Chemical Engineers to exploit the intellectual property. This enables these organisations to make these documents available and also update them as deemed appropriate.

The technical volumes outline the latest science in the field of natural hazard characterisation and are supported by case studies that illustrate how these approaches can be used to better understand the risks posed to UK infrastructure projects. The documents presented are split into a set of eleven technical volumes and five case studies.

Each technical volume aims to provide an overview of the latest science available to characterise the natural hazard under consideration within the specific volume. This includes a description of the phenomena related to a natural hazard, the data and methodologies that can be used to characterise the hazard, the regulatory context and emerging trends. These documents are aimed at the technical end-user with some prior knowledge of natural hazards and their potential impacts on infrastructure, who wishes to know more about the natural hazards and the methods that lie behind the values that are often quoted in guideline and standards documents. The volumes are not intended to be exhaustive and it is acknowledged that other approaches may be available to characterise a hazard. It has also not been the intention of the project to produce a set of standard engineering 'guidelines' (i.e. a step-by-step 'how to' guide for each hazard) since the specific hazards and levels of interest will vary widely depending on the infrastructure being built and where it is being built. For any energy-related projects affected by natural hazards, it is recommended that additional site- and infrastructure-specific analyses be undertaken by professionals. However, the approaches outlined

aim to provide a summary of methods available for each hazard across the energy industry. General advice on regulation and emerging trends are provided for each hazard as context, but again it is advised that end-users investigate in further detail for the latest developments relating to the hazard, technology, project and site of interest.

The case studies aim to illustrate how the approaches outlined in the technical volumes could be applied at a site to characterise a specific set of natural hazards. These documents are aimed at the less technical end-user who wants an illustration of the factors that need to be accounted for when characterising natural hazards at a site where there is new or existing infrastructure. The case studies have been chosen to illustrate several different locations around the UK with different types of site (e.g. offshore, onshore coastal site, onshore river site, etc.). Each of the natural hazards developed in the volumes has been illustrated for at least one of the case study locations. For the sake of expediency, only a small subset of all hazards has been illustrated at each site. However, it is noted that each case study site would require additional analysis for other natural hazards. Each case study should be seen as illustrative of the methods outlined in the technical volumes and the values derived at any site should not be directly used to provide site-specific values for any type of safety analysis. It is a project recommendation that detailed site-specific analysis should be undertaken by professionals when analysing the safety and operational performance of new or existing infrastructure. The case studies seek only to provide engineers and end-users with a better understanding of this type of analysis.

Whilst the requirements of specific legislation for a sub-sector of energy industry (e.g. nuclear, offshore) will take precedence, as outlined above, a more rounded understanding of hazard characterisation can be achieved by looking at the information provided in the technical volumes and case studies together. For the less technical end-user this may involve starting with a case study and then moving to the technical volume for additional detail, whereas the more technical end-user may jump straight to the volume and then cross-reference with the case study for an illustration of how to apply these methodologies at a specific site. The documents have been designed to fit together in either way and the choice is up to the end-user.

The documents should be referenced in the following way (examples given for a technical volume and case study):

ETI. 2018. *Enabling Resilient UK Energy Infrastructure: Natural Hazard Characterisation Technical Volumes and Case Studies,* Volume 1 — Introduction to the Technical Volumes and Case Studies. IMechE, IChemE.

ETI. 2018. *Enabling Resilient UK Energy Infrastructure: Natural Hazard Characterisation Technical Volumes and Case Studies,* Case Study 1 — Trawsfynydd. IMechE, IChemE.

Contents

Case Study 1: Trawsfynydd

Contents

1. Introduction

This case study illustrates the appropriate use of the derived methodology for Trawsfynydd, Wales. Trawsfynydd is located in North Wales and is the site of a nuclear energy plant (currently being decommissioned). The site was chosen as representative of an inland site.

Three hazard families are included in this assessment:
- Volume 2 — Extreme High and Low Air Temperature;
- Volume 7 — Seismic, Volcanic and Geological Hazards;
- Volume 12 — Hazard Combinations.

The specific methodologies applied are described in the individual guideline documents associated with each of the three hazard families.

1.1   Site geography and geology

Trawsfynydd is a village located in Gwynedd, North Wales, 16 kilometres (km) from the coast, in the central part of the Snowdonia National Park (*see Figure 1*). The closest towns are Porthmadog on the coast to the west (~15 km, along the A487), Blaenau Ffestiniog to the north (~10 km, along the A470), Bala to the east (~20 km, along the A494) and Dolgellau to the south (~20 km, along the A470).

A man-made reservoir, Llyn Trawsfynydd or Lake Trawsfynydd, is located next to the village. It has an altitude of 196 metres (m) above sea level, a maximum length of about 4 km, and an area of 5.3 km^2. The mean depth of the lake is 5.2 m but reaches 9 m over a very small part near the dam. The lake catchment is 92 km^2 and is mostly fed by the Afon Prysor (*Whitehouse, 1971*), with smaller contributions from various streams which drain the surrounding hills. The outflow eventually joins the river Dwyryd which in turn flows into the estuary near Porthmadog.

The area is surrounded by mountains to the north (around Blaenau Ffestiniog, maximum elevation ~770 m), the west and south-west (Rhinogs range, maximum elevation ~700 m) and east and south-east (Arenig range, maximum elevation ~850 m). The Rhinogs shelter Trawsfynydd from the prevailing south-westerly winds. Land use is a mix of farmland, wilderness, woodland, and a few large forests (Coed y Brenin between Trawsfynydd and Dolgellau; Gwydir north-east of Blaenau Ffestiniog).

The underlying geology of the locality is typified by shallow Cambrian bedrock (*Figure 2*), with the majority comprising thick bedded turbiditic sandstones, conglomerates and laminated sandstones, mudstones, and occasional intrusive volcanic dykes. Superficial deposits are absent

in many areas, but where present they comprise glacial till (diamicton clay), with localised areas of peat deposits, particularly to the south. The UK experiences a relatively low level of seismic activity overall, and most of this activity is located in North Wales, with earthquakes occurring more frequently in the region than other areas of the UK.

Figure 1. Map indicating the location of the Trawsfynydd site along with closest towns, nearby landmarks (mountain ranges and major forests) and weather observation stations. Contains OS data © Crown copyright and database right (2018)
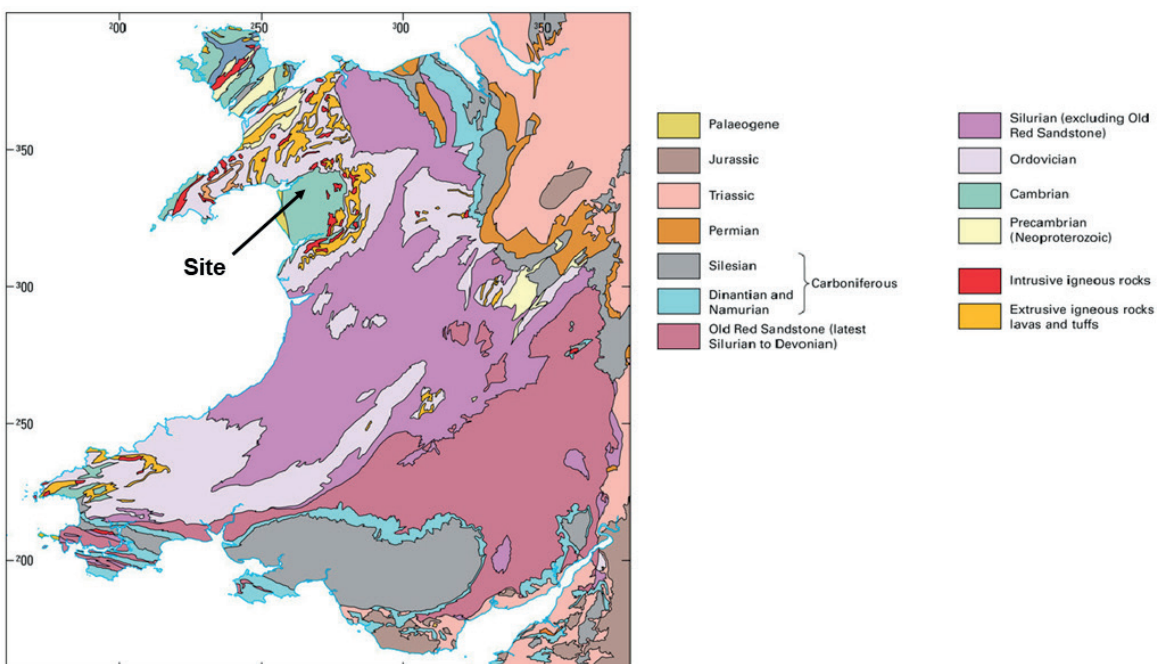

Figure 2. Solid geology of Wales. (Reproduced with the permission of the British Geological Survey ©NERC. All rights reserved.)

1.2 Site industrial history

Past industrialisation in North Wales pertained to slate quarries. Nowadays, the main components of its economy are tourism and public services, with for example several slate quarries now used for tourism-based businesses. The nearest harbour, Porthmadog, is mainly used for leisure and fishing.

Llyn Trawsfynydd was created between 1924 and 1928 to supply water for the Maentwrog hydroelectric power station downstream the Afon Prysor. Four dams were constructed; the main one (Maentwrog dam) was at the time the largest arch dam to be built in Britain with a height of 29 m and a width at the base of 11 m (*Coflein, 2018*). The dam was rebuilt in 1987. A nuclear power station was built on the north side of Llyn Trawsfynydd (site coordinates: 52° 55' 35" N, 3° 56' 46" W, OS grid reference SH 69270 38343). The power station was operated by Magnox Ltd (it was the first inland civil Magnox nuclear station) and was in service from 1965 to 1991, generating a total of 69 terawatt hours. The height of Maentwrog dam was raised in the early 1960s to supply adequate water for both the hydroelectric plant and the nuclear power station. Some additional work was carried out to channel the water into and out of the station, ensuring as much time as possible for the heated water discharged to cool (*Whitehouse, 1971*). The site continues to be managed by Magnox Ltd; the power station was permanently shut down in 1993 and is in the process of being decommissioned. It is currently undergoing an accelerated entry to the Care and Maintenance Preparations phase (*Magnox, 2018*). The Maentwrog hydroelectric plant remained operational whilst the nuclear power station was in service, and is still operating today.

1.3 Site climatology

Trawsfynydd experiences a maritime climate much like the rest of the UK, with prevailing winds coming from the Atlantic Ocean.

The annual climatologies of temperature, rainfall and wind are shown in *Figure 3* and *Figure 4*. Climatologies are long-term averages considered representative of the state of the climate in the region. Temperature and rainfall climatologies cover the 30-year period of 1981 to 2010 and are provided for Trawsfynydd and the two neighbouring weather stations of Porthmadog and Bala (see *Figure 1* for location and *Section 2.1.2* for more details). As the weather station in Trawsfynydd stopped recording data in 1998 and the weather station in Porthmadog operated from 1993 only, missing data have been estimated (where possible) using a linear regression from overlapping data periods with up to six well-correlated neighbouring weather

stations (*Perry and Hollis, 2005*). The wind rose covers the period of 1981 to 1998 and is for Trawsfynydd only.

These climatologies show that July and August are the warmest months at Trawsfynydd with a mean daily temperature of 16 °C (mean daily maximum temperature of 18 °C). December, January and February are the coldest months with a mean daily temperature of 4 °C (mean daily minimum temperature of 1 °C). The effect of the proximity of the sea to the weather station is noticeable, with Porthmadog experiencing warmer temperatures compared to Trawsfynydd and Bala. The autumn and winter are wetter than the spring and summer; and the prevailing wind direction is from the south-west, with maximum hourly mean wind speeds of over 33 knots (17 metres per second (m/s) or 38 miles per hour (mph)). Trawsfynydd also appears to receive more rainfall on average, a phenomenon likely due to orographic effect, i.e. moist air forced upwards when it travels over higher ground, producing cloud and potentially rainfall (*Met Office, 2017b*).
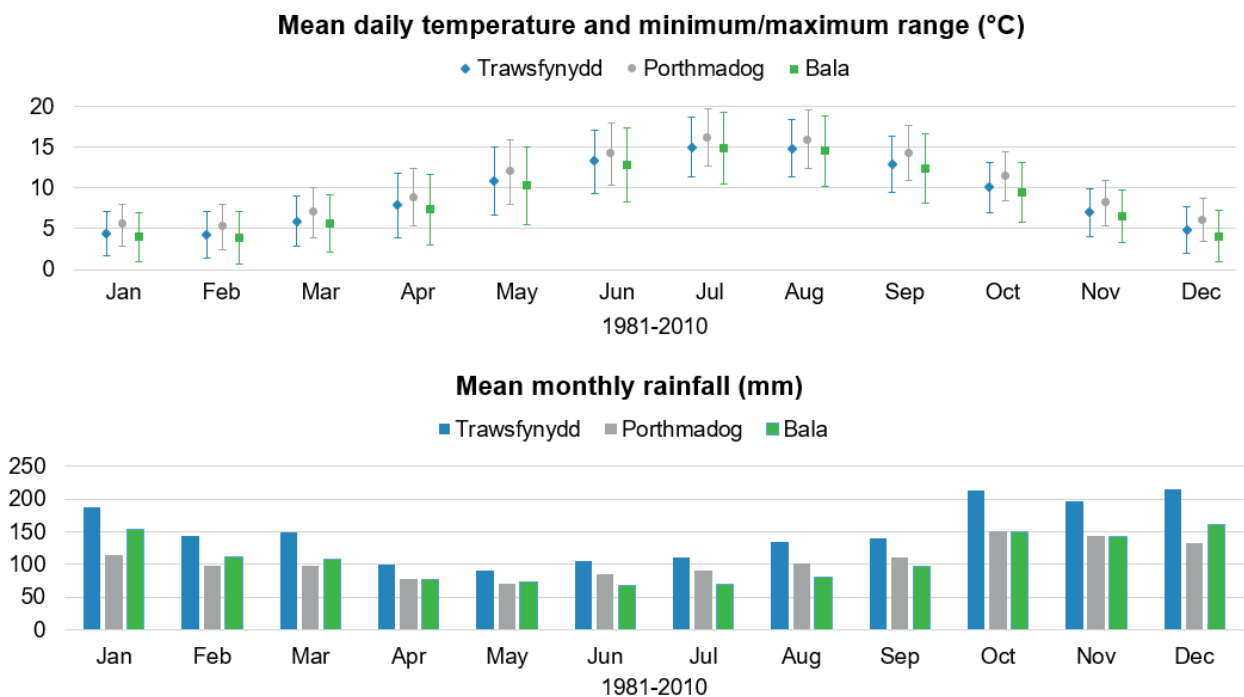
Figure 3. Climatology of daily mean, minimum and maximum temperatures and of monthly rainfall for the weather stations indicated on the graphics, for the period of 1981 to 2010. Missing data for Trawsfynydd (from 1998) and Porthmadog (before 1993) were estimated (where possible) using a linear regression from overlapping data periods with up to six well-correlated neighbouring weather stations following the approach of Perry and Hollis (2005).

Figure 4. Climatology of wind speed and direction for Trawsfynydd weather station for the period of 1981 to 1998.

Ground frost, defined as a minimum grass temperature below 0 °C, typically occurs from November to April with an average twelve to sixteen days per month, but can be observed as early as September and as late as June. There are about four to five days of snow lying on the ground per month from December to February, but snow on the ground can be observed as early as November and as late as May. Some extremes for Trawsfynydd are listed in *Table 1*. Temperature extremes are discussed in depth in *Section 2.1*.

Table 1. Local weather extremes at Trawsfynydd over the record period (1960 to 1998). Source data: © Crown copyright Met Office 2018.

Trawsfynydd	Value	Date
Temperature		
Highest daily temperature	31.5 °C	2nd Aug 1990
Lowest daily temperature	−11.1 °C	19th Nov 1962
Rainfall		
Maximum daily rainfall total	90 mm	21st Nov 1980
Maximum hourly snow depth	30 cm	11th Dec 1967
Wind speed		
Maximum hourly gust speed	39 m/s (87 mph)	15th Jan 1993

Three families of natural hazards are considered at Trawsfynydd: extreme temperatures; seismic, geological and volcanic hazards; and natural hazard combinations. Other families of natural hazards are relevant at the site but are not part of this case study.

For background information, the reader should refer to the corresponding technical volumes:
- Volume 2 — Extreme High and Low Air Temperature;
- Volume 7 — Seismic, Volcanic and Geological Hazards;
- Volume 12 — Hazard Combinations.

2.1   Extreme temperatures

In this case study, the term extreme temperatures encompasses extreme high air temperatures, extreme low air temperatures, rapid changes in air temperature, extreme water temperatures, frazil ice, and wildfires. The focus of this section is extreme air temperature (maximum and minimum), with analysis and detailed discussion presented below; a brief discussion, with no analysis, is provided for the remaining topics.

2.1.1   Impacts

Extreme high and low air temperatures

There is no universal definition of an extreme air temperature (see Section 1 of Volume 2 — Extreme High and Low Air Temperature). An extreme temperature is understood to be an event that occurs infrequently and as a result there are often very few data available to study these events. Different approaches are used to describe extreme events. These include using a predefined percentile of the historical record (e.g. an event of greater magnitude than the 98th percentile, see *Sanderson et al. (2017)*), or an operational threshold specific to a particular part of the energy sector.

Extreme air temperatures can have a diverse range of impacts on the energy industry. For example, high temperatures can decrease the effectiveness of steam turbines in some power stations or the cooling capacity of HVAC units. In some circumstances, high temperatures can enhance biological growth in water, which may lead to blocking of the cooling water intake.

The International Electrotechnical Commission requires all outdoor electrical components to function in ambient temperatures of −25 °C to 40 °C, values which correspond approximately to the range of recorded UK air temperatures, −27.2 °C to 38.5 °C. However, the current observed maximum temperature is taken from thermometers inside a Stevenson screen (see Volume 2 — Extreme High and Low Air Temperature). The location and the design of the

Stevenson screen is such that the temperature measured is unaffected by thermal radiation and moisture, and air is allowed to circulate freely. This temperature could be appreciably different to that experienced by the outdoor equipment (reasons for this include direct exposure to the sun, position of the equipment in relation to buildings, and whether the equipment is sheltered from winds).

Extreme low temperatures can also cause a number of issues, either on their own or in combination with other meteorological variables such as precipitation. For instance, heavy snowstorms or ice storms can load extra weight on infrastructure such as power lines, freeze structures, and physically block roads or access to power plants. Hazard combinations and the characterisation of hazard combinations are discussed in more detail in *Section 2.3*.

Rapid changes in air temperatures

The definition of what constitutes a rapid change in air temperature is likely to be specific to each part of the energy sector. There are a number of temporal scales that could be considered, such as rapid increase/decrease on a sub-hourly or hourly scale through to large diurnal changes.

Provided that suitable data exist at the desired temporal scale, it would be possible to analyse extreme rapid changes in air temperature using a similar approach to that taken in *Section 2.1.3* for the extreme minimum and maximum air temperatures.

Extreme water temperatures

The effect of the power station on the lake was studied in the late 1960s (*Whitehouse, 1971*). The study provided monthly means of the lake's surface water temperatures in 1963 and 1964 (before the nuclear power station started operating). The water temperatures oscillate on average between 6 °C and 17 °C (winter and summer respectively). In the present-day climate, these temperatures may be on the lower side due to global warning. *Woolway et al. (2017)* gives a warming rate of 0.55 °C per decade for lakes in Europe based on surface water temperatures from 1996 to 2015, assuming a linear trend.

Given this temperature profile, extreme high lake temperatures are very unlikely to be an issue for cooling purposes of a power station. For a reactor to be cooled safely and effectively, coolant water temperatures should not exceed temperatures of 28 °C and must also be returned to the water body within an environmentally safe temperature limit (e.g. *Defra (2010)*). Water temperatures can sometimes exceed this environmental safety limit, especially over a period of consecutive days of high air temperatures. For instance, the 2003 heatwave across Europe caused several

nuclear power stations in France to operate at reduced capacity or be shut down, because the river water level dropped so low that the cooling process was impossible, or because temperatures, after the cooling process exceeded environmental safety limits (*The Guardian, 2003; UNEP, 2004*). However, these power stations were river-cooled, while any facility at Trawsfynydd would need to use the water of Llyn Trawsfynydd. In the case of this lake, the water is thought to be thoroughly mixed; it is also not naturally stratified during the summer because rapid mixing is induced by the lake's relative shallowness with respect to its surface area and the presence of high wind speeds. Only under particular conditions of low wind speed and high sunshine could thermal stratification of the lake then be possible (the surface waters, heated by the sun, stay on top of the deeper, cooler waters, as warmer water is less dense). This stratification could then potentially be an issue for cooling purposes of a power station. As explained in detail in Volume 11 — Marine Biological Fouling, extended days of extremely high temperatures may cause algal growth which may in turn clog water intakes. These algal blooms are more likely to occur under high temperature conditions and with sluggish water circulation, especially in 'closed' systems such as lakes.

Extreme low lake temperatures are unlikely to be an issue at the site. Temperatures in the UK are rarely low enough for long enough to cause lakes to freeze all the way to depth. December 2010, the coldest December in over 100 years (*Met Office, 2011*), caused the freezing of only the surface of Derwentwater in Cumbria (*Jamieson, 2010*).

Frazil ice

Frazil ice is the first stage of the formation of ice in oceans and rivers. In rivers, it typically forms in turbulent water bodies when the water is supercooled to temperatures below −0.01 °C with ambient air temperatures of about −6 °C (*Schaefer, 1950*). Sea water has a lower freezing point of −1.8 °C due to the salinity of the water. Frazil ice is uncommon in the UK but not unheard of. It was reported on the River Dee in December 2014, where 'ice pancakes' formed due to the movement of water which prevented the ice from forming a flat sheet (*BBC, 2014*).

Wildfires

In the UK, wildfires occur during the spring and summer on moorlands, heaths, grassland, forest/ woodland and agricultural land, and are primarily started by people, whether accidentally or deliberately. The majority tend to be small incidents, but some may evolve into major incidents when a large amount of dry or dead vegetation is present on the ground (spring) and in warm, dry and windy weather (spring, summer).

Wildfire damage is caused through fire, heat and smoke. Therefore, factors such as location of, and proximity to, an ongoing wildfire would need to be considered in assessing impacts for the site, as well as typical weather (in particular, the prevailing wind direction).

The Welsh Government publishes annual grassland fire statistics (*Welsh Government, 2018*). It states that Welsh Fire and Rescue Authorities attend an average of 14,500 (reported) fire incidents per year, with about 25% being wildfires (grassland, woodland, crop; numbers valid since the financial year 2009/2010). In the financial year 2016/2017, there were 1716 wildfires, three in five damaging an area of less than 20 m^2 and one in six more than 200 m^2 (*Welsh Government, 2017*). The majority occurred on grassland, heathland, moorland and scrub land; woodland/forest fires accounted for 1% of all wildfires, but were all primary fires (i.e. involving casualties/rescue or attended by at least five appliances). Three quarters were started deliberately and approximately 20% were located in North Wales (8% of the latter were primary incidents). According to the Welsh Government wildfire statistics (covering the period 2000 to present), wildfires have occurred within a few kilometres of Trawsfynydd. In fact, there have been three primary fires close to the site since 2006 and a handful of secondary fires most years since 2011 (i.e. not involving casualties/rescue or attended by fewer than five appliances; these were mainly grass fires).

2.1.2 Data and history

As mentioned previously, *Section 2.1* discusses natural hazards related to extreme temperatures. From this point onwards, the focus is on extreme air temperature at Trawsfynydd, with a discussion of data availability and suitability as well as history of extreme events, and with a detailed analysis of extreme air temperatures for Trawsfynydd.

Ideally, a long record of data is needed if an accurate estimate of the severity of extreme events is required. Such record increases the probability of sampling very rare events, and if suitably long, can take into account naturally-varying climatological oscillations, such as the *North Atlantic Oscillation** (NAO).

Three weather stations have been considered in this case study: Trawsfynydd, Porthmadog and Bala (locations indicated in *Figure 1* and details available in *Table 2*). A single one has been selected to reduce the complexity of the analysis (see Section 4 of Volume 2 — Extreme High and Low Air Temperature).

*All technical terms marked in blue can be found in the Glossary section.

Case Study 1: Trawsfynydd

Table 2. Details of weather stations at or near Trawsfynydd. Source data: © Crown copyright Met Office 2018.

Station	Location	Elevation above sea level	Availability of temperature measurements
Trawsfynydd	52.93°N, 3.94°W	193 m	1960 to 1995
Porthmadog	52.91°N, 4.16°W	7 m	1993 to present
Bala	52.91°N, 3.58°W	163 m	1970 to present

The weather station selected to represent the site of Trawsfynydd in this demonstration is Bala because of its slightly longer temperature record and because the extreme percentiles seem fairly consistent (a difference of approximately 0.6 °C; see *Table 3*) even if it experiences slightly warmer temperatures than Trawsfynydd. Porthmadog was discarded as its climate is milder than that of inland sites due to its proximity to the sea (as discussed in *Section 1.3*) and this holds when comparing extreme temperatures between the stations (see *Table 3*).

The time series of extreme maximum and minimum temperatures for Bala are shown in *Figure 5*. These exhibit some variability from year to year, but while it is difficult to discern any long-term trend in the values shown there is some evidence for a trend in the 30-year means for 1971 to 2000 and 1981 to 2010 shown in *Figure 6*. Indeed, the distributions for 1981 to 2010 are slightly skewed towards higher minimum and maximum temperatures than those for 1971 to 2000.

Table 3. Extreme percentiles of maximum temperature calculated from the daily data.
The numbers in brackets represent the difference between the selected station and Trawsfynydd.

Percentile	Porthmadog (°C)	Trawsfynydd (°C)	Bala (°C)
95	22.1 (0.8)	21.3	21.8 (0.5)
96	22.8 (0.9)	21.9	22.5 (0.6)
97	23.7 (1.1)	22.6	23.3 (0.7)
98	24.7 (1.0)	23.7	24.3 (0.6)
99	26.5 (1.4)	25.1	25.7 (0.6)
99.2	27.1 (1.5)	25.6	26.2 (0.6)
99.4	27.6 (1.6)	26.0	26.7 (0.7)
99.6	28.3 (1.3)	27.0	27.3 (0.3)
99.8	29.4 (1.4)	28.0	28.6 (0.6)
99.9	30.7 (2.0)	28.7	29.3 (0.6)
100 (most extreme event)	34.5 (3.0)	31.5	32.3 (0.8)

Daily maximum temperature (°C)

Daily minimum temperature (°C)
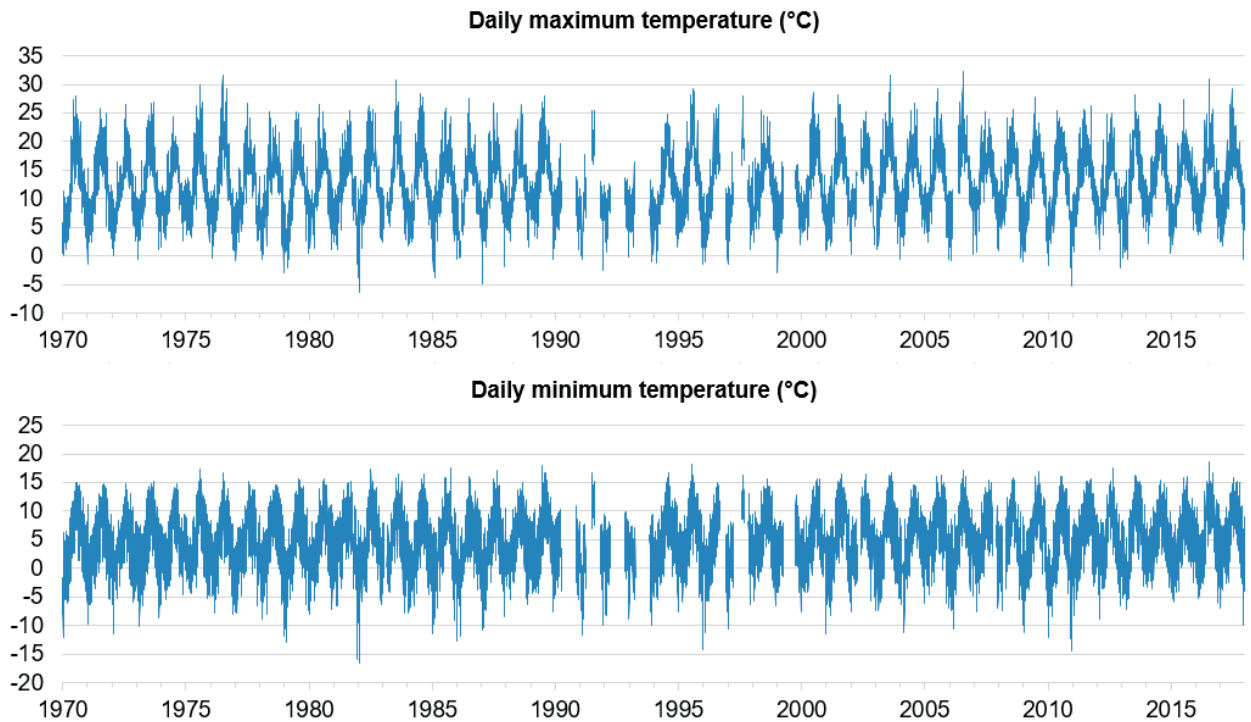
Figure 5. Time series of available daily maximum and minimum temperatures at Bala. Some periods in the 1990s were unavailable due to an operational hiatus.

30-year mean minimum daily temperature (°C)

■ 1971-2000 ■ 1981-2010

30-year mean maximum daily temperature (°C)

■ 1971-2000 ■ 1981-2010
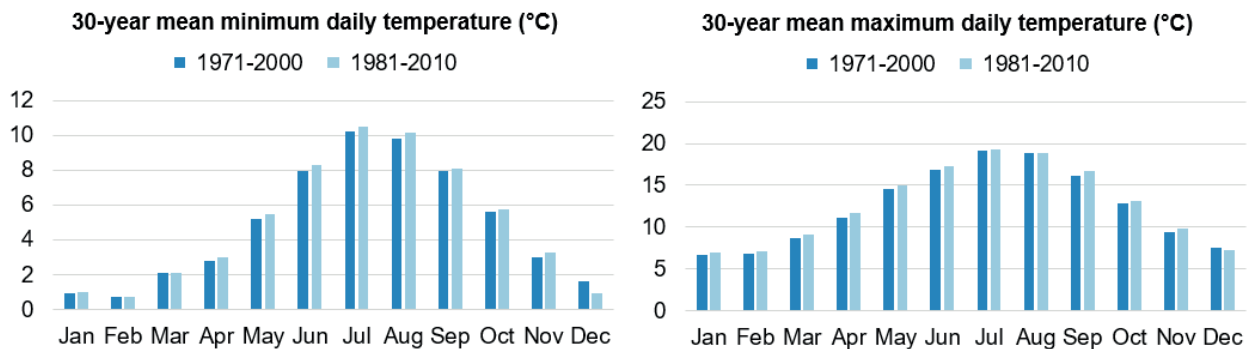
Figure 6. Climatological daily minimum and maximum temperatures at Bala for the 30-year periods 1971 to 2000 and 1981 to 2010.

Table 4 shows the ten hottest and coldest days at Bala. Many of the extreme values are on a day adjacent to another extreme value within both the maximum and minimum top ten. Examples include 12th to 15th January 1982 in the minimum temperatures (ranks number 5, 4, 2 and 1) and 18th to 19th July 2006 in the maximum temperatures (ranks number 9 and 1). This suggests that neither the daily maximum temperatures nor the daily minimum temperatures are independent of one another.

Case Study 1: Trawsfynydd

Meteorologically, the winter of 1981 to 1982 had a prolonged period of extremely cold temperatures. The extreme cold was caused by an anticyclone (high-pressure system) centred over Scandinavia and bringing cold and moist air over the UK; this lasted for ten days (*Roach and Brownscombe, 1984*). The warm extremes of 18th to 19th July 2006 were associated with an anticyclonic weather pattern that became established over the UK and the North Sea from 13th July onwards (*Prior and Beswick, 2008*). The hot, dry summer of 1976 and the extremely cold month of December 2010 are also reflected in the values.

Table 4. Top ten coldest and hottest days at Bala. © Crown copyright Met Office 2018.

Rank	Top ten hottest days at Bala (°C)		Top ten coldest days at Bala (°C)	
1	32.3	19th Jul 2006	−16.5	15th Jan 1982
2	31.7	9th Aug 2003	−16.2	14th Jan 1982
3	31.6	3rd Jul 1976	−16.0	13th Dec 1981
4	31.3	29th Jun 1976	−15.9	12th Jan 1982
5	30.9	19th Jul 2016	−14.6	13th Jan 1982
6	30.8	12th Jul 1983	−14.5	19th Dec 2010
7	30.6	11th Jul 1983	−14.4	20th Dec 2010
8	30.5	2nd Jul 1976	−14.3	28th Dec 1995
9	30.5	18th Jul 2006	−13.9	21st Dec 2010
10	30.4	4th Jul 1976	−13.4	12th Dec 1981

2.1.3 Methodology

Several methodologies exist to assess temperatures at a location based solely on the observed events; these are discussed in Volume 2 — Extreme High and Low Air Temperature. The methodology selected for demonstration in this case study is an extreme value analysis (EVA). This was selected because, unlike the other methodologies, it allows one to quantify robustly the most extreme values in the observational record and to extrapolate out to extreme levels beyond those seen in the observational record. The EVA does so by inferring a return level associated with an annual exceedance probability (AEP). A return level is the value that has the specified probability of being exceeded in a given period. The return period is the inverse of the AEP.

Within an EVA, various approaches coexist and are selected based on the nature of the extreme events to characterise. In this case study, a generalised extreme value (GEV) distribution is applied to the most extreme maximum temperatures in a calendar year (block maxima approach), while a Poisson-generalised Pareto distribution (PP-GPD) is used to analyse extreme daily minimum temperatures (threshold exceedance model).

Note that there is no physical or statistical reason why the daily maximum temperatures cannot be analysed using a threshold exceedance approach. In this section, it was considered desirable to demonstrate both approaches. Both approaches are implemented with the extRemes 2.0 EVA package in the statistical programming language R (*Gilleland and Katz, 2016*).

Note on climate change

For simplicity, it is assumed in this analysis that the observations of maximum and minimum temperatures at Bala are stationary, i.e. there is no long-term trend within the data (even if in the case of Bala there is evidence against this). Section 7 of Volume 2 — Extreme High and Low Air Temperature discusses climate change in more detail and provides references to the literature that discuss how to incorporate non-stationarity into an EVA.

Daily maximum temperatures

Selecting extreme maximum temperatures

Figure 7 shows a time series of the largest extreme value for each month for the maximum daily temperature record for Bala. Although data from the Met Office archive are automatically quality-checked, a further look at the values is required to ensure they are as accurate as possible. The most extreme events look realistic within the context of extreme temperatures experienced within the UK and therefore for Wales (see Section 1 of Volume 2 — Extreme High and Low Air Temperature). However, this figure highlights several potential issues with the data which must be resolved prior to the EVA.

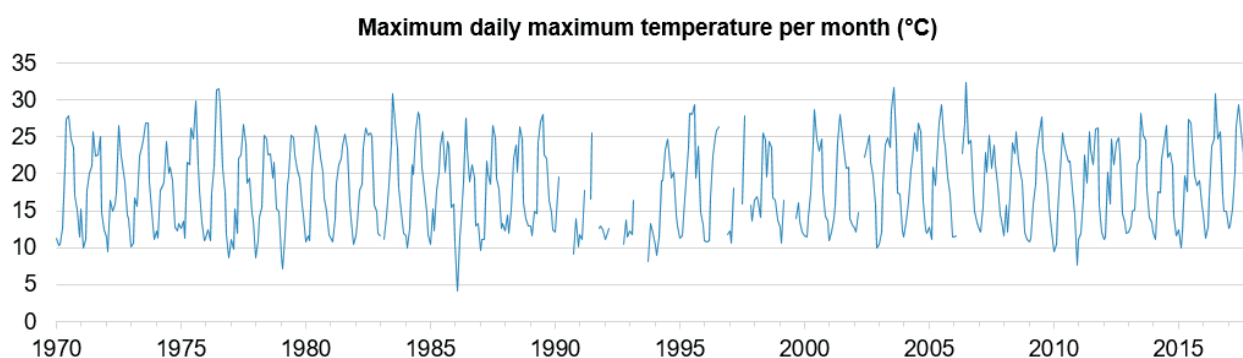*Figure 7. Largest daily temperature observed at Bala for each month from 1970 to 2017.*

The maximum temperature of less than 5 °C in February 1986 appears atypical and could warrant further research. Sometimes, outlying values can occur if only a subset of values have been recorded in a month. A detailed look at the record proved that this is not the case for February 1986 (temperatures were indeed particularly cold that month).

Several periods of data are missing in the 1990s. They could cause an issue especially if missing during the typical hottest months of the year (July and August), and could result in any estimates of the return levels being too low. For this reason, each whole year is excluded from the record to be analysed if any of its summer months (June to August) has fewer than 25 recorded maximum temperature observations. This led to the exclusion of 1990, 1991, 1992, 1993, 1996, 1997 and 1999. It is also implicitly assumed that if a summer month has 25 or more observed records, but fewer than the total number of days in the month, then the hottest day of the year does not occur on the missing day.

This provided a set of 41 extreme high temperatures (one per valid year).

Fitting a GEV model

The estimated location, scale and shape parameters of the fitted GEV distribution are listed in *Table 5*, along with their uncertainty. Hereafter, the confidence intervals are generated via the profile-likelihood approach, unless specified otherwise (see *Coles (2001)* and Section 4 of Volume 2 — Extreme High and Low Air Temperature for further information).

Table 5. Estimated location, scale and shape parameters of the fitted GEV distribution.

	Location	Scale	Shape
Estimated value	26.31	1.46	0.13
Standard error	0.27	0.21	0.17
95% normal-approximated confidence interval	[25.77, 26.84]	[1.04, 1.88]	[−0.20, 0.45]
95% profile-likelihood confidence interval	[25.81, 26.89]	[1.11, 1.97]	[−0.17, 0.48]

Diagnostic plots for the GEV distribution fitted to the annual maximum temperatures are shown in *Figure 8* (see Volume 2 — Extreme High and Low Air Temperature for further information on diagnostic plots).

The probability and quantile plots help to assess how well the distribution fits the data. A perfect fit would result in a match of the probabilities (or quantiles) of the statistical model to the observed (empirical) probabilities (or quantiles), i.e. all the points would lie on the 1:1 (diagonal) line in each plot. The probabilities and the quantiles lie here close to this 1:1 line, suggesting that the distribution is a reasonable representation of the annual extreme values.

The quantile plot indicates a very close agreement of the empirical quantiles to the GEV quantiles up to 29 °C, but at higher temperatures the GEV quantiles may be underestimated. However, some slight deviation of the empirical quantiles from the 1:1 correspondence line is not unusual for the highest quantiles and can occur due to sampling error. Sampling error is the difference between a 'true' value, in this case the population value for the percentile, and an estimate derived from a random sample. Sampling errors occur because a sample of values is observed, not the entire population; they are not due to imperfect selection, bias in response or estimation, errors of observation and recording, etc.

The density plot (also known as probability density plot) compares the empirical probability density derived from the data to the probability density derived from the GEV distribution with the parameters for location, scale and shape of *Table 5*. Both the empirical and GEV curves are in relatively good agreement with each other, a suggestion again that the GEV is a reasonable model for the annual maximum temperatures. The 'bulge' in the observed curve around 32 °C could be due to sampling error, or could suggest that there is a physical process not considered in the fitted GEV model and associated with the most extreme annual temperature events. A tally of the annual maximum data shows that there are only three values greater than 31 °C, and only one of these is greater than 32 °C, suggesting that the 'bulge' is more likely to be attributable to sampling error.
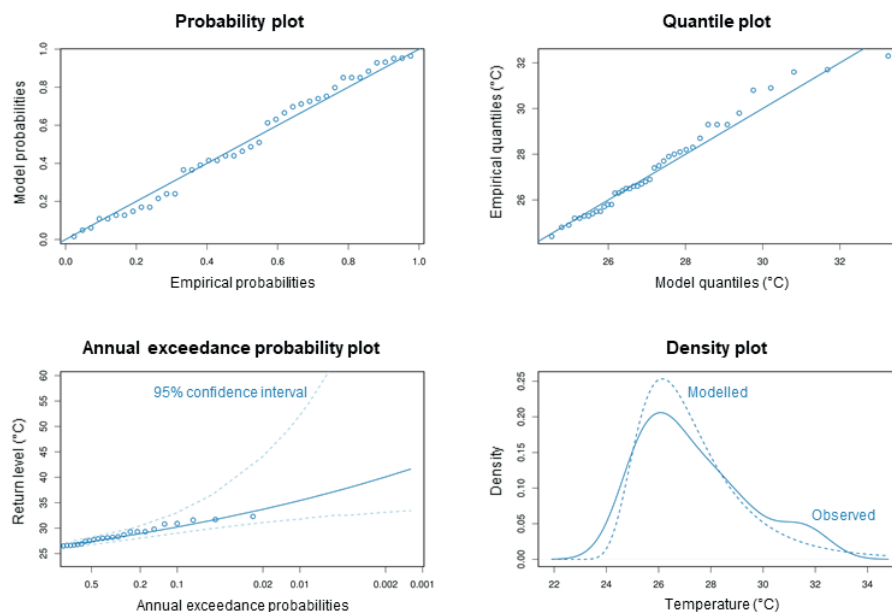

Figure 8. Standard diagnostic plots of the fit of the GEV distribution to the annual maximum temperatures at Bala.

Calculating return levels

Overall, the diagnostic plots for the GEV model suggest that the model is a good fit to the annual maximum temperatures, lending confidence to using the model to calculate annual exceedances for return levels of extreme maximum temperatures.

Table 6 lists return levels for a number of AEPs. The smaller the exceedance probabilities, the greater the uncertainty about the return level, a behaviour also noticeable in the annual exceedance plot of *Figure 8* where the 95% confidence interval around the extreme temperatures (return levels) widens as the AEP decreases (return period increases; the return period is the inverse of the AEP). Therefore, caution is urged when using very small AEPs, particularly when the return period extends appreciably beyond the length of the time series used to fit the GEV distribution.

Table 6. Return levels for a selection of AEPs along with associated 95 % profile-likelihood confidence limits for extreme maximum temperatures at Bala, calculated from the fitted GEV distribution.

AEP		Temperature	95% confidence interval
0.5	(2-year return period)	26.9 °C	[26.2 °C, 27.5 °C]
0.05	(20-year return period)	31.6 °C	[30.2 °C, 36.6 °C]
0.01	(100-year return period)	35.4 °C	[33.0 °C, 45.3 °C]

The upper limit for the 95% confidence interval for the AEP of 0.01 is found to be greater than 38.5 °C, the current hottest observed temperature in the UK. This high upper confidence limit could be a result of the very small number (41 values) of extreme temperatures available for Bala. There are some limitations associated with using only the annual maximum temperatures (block maxima approach), e.g. other extreme values in the same year are ignored. Using a threshold exceedance model would help to overcome these limitations and could result in a lower value for the upper 95% confidence limit of the AEP of 0.01.

Daily minimum temperatures

The analysis of the fit of a PP-GPD to the minimum temperatures is presented in three parts, each building upon the statistical model presented in the previous part.
- Part 1: Fitting a PP-GPD model
- Part 2: Including a covariate for the NAO
- Part 3: Removing correlated extreme values

Part 1 is similar to the preceding GEV analysis in that the appropriateness of the fit of the PP-GPD is assessed using diagnostic plots. Parts 2 and 3 build upon this first basic model in order to improve its specification and allow the calculation of return levels.

Parts 2 and 3, as well as the return level calculations, touch on the degree of statistical complexity that can be required when fitting and assessing statistical models to extreme meteorological data and interpreting the results.

Selecting extreme minimum temperatures

Unlike the block maxima approach, the threshold approach considers all observations beyond a prescribed threshold, including potentially informative but less extreme events.

A range of thresholds was investigated to select the minimum temperature events. The sensitivity analysis pointed to the most suitable threshold being −7.7 °C, which provides 129 extreme minimum temperature events.

As these events include negative values and as the extreme value distributions and EVA theory have been developed to model maximum extremes, all selected extreme minimum temperatures are here multiplied by −1. From this point onwards, please note that figures make use of this transformed scale (unless otherwise indicated), but that citations of values in the text are on the original scale.

Part 1: Fitting a PP-GPD model

The diagnostic plots of the fit of the PP-GPD are shown in *Figure 9*.

In the probability and density plots, any appreciable deviation from the 1:1 line could indicate that the fitted extreme value distribution may not represent the observed data well. The concave nature of the probability plot here suggests that the main body of the data has lower temperatures (is to the left) compared to the fitted model, a result also observed in the density plot. The quantile plot magnifies any differences between the tails of the fitted and observed distributions. In the present case, there appears to be some deviation between the observed and fitted model in the tails.

The plot of AEPs also suggests differences between the observations and the fitted model, as most points lie outside the lower bounds of the 95 % confidence interval for high AEPs. The density plot further highlights the mismatch between the observed distribution and that of the fitted PP-GPD model.

As it is currently specified, the PP-GPD model is clearly a poor fit for the data and therefore does not represent adequately the observed extreme minimum temperatures at Bala. The density plot points to a bimodality of the observations, for which one possible explanation is the influence of the NAO, a pattern of pressure variability over the North Atlantic, usually described as a pressure difference between the usually low pressure over Iceland and the usually high pressure over the Azores (see Section 2 of Volume 2 — Extreme High and Low Air Temperature). The NAO influences the winter climate of the UK; it moves between positive and negative phases. In the positive phase, the winter usually is stormier and milder; in the negative phase, the winter usually is calmer and colder (see Section 2 of Volume 2 — Extreme High and Low Air Temperature). Note that a positive NAO phase does not exclude the possibility of observing an extreme minimum temperature.

Figure 9. Diagnostic plots of the fit of the PP-GPD distribution to the extreme minimum temperatures at Bala. The confidence intervals are approximate 95% normal confidence intervals. Note that the minimum temperatures displayed are on a transformed scale (i.e. multiplied by −1).

Part 2: Including a covariate for the NAO

In order to specify better the PP-GPD statistical model for the extreme minimum temperatures at Bala, daily observations of the NAO index are included as a covariate in the model for the location parameter.

The diagnostic plots in *Figure 10* suggest that a PP-GPD with NAO as a covariate is a better fitting

model compared to the PP-GPD without a covariate. In both the probability plot and quantile plot points lie closer to the 1:1 correspondence line compared to *Figure 9* (note the change in the scale for the quantile plots). The reader will note that since the AEPs are now dependent on both the frequency (or rarity) of the extreme temperatures and the NAO phase, the probability plot and the quantile diagnostic plots now focus on the residuals (*Coles, 2001*).

The Z plot highlights that the PP-GPD model is not yet correctly specified for there to be high confidence in any return levels associated with the AEPs, as there is an appreciable difference between the 1:1 correspondence line and the fitted line. Indeed, the Poisson component of the PP-GPD models the frequency of the extreme events, and if observations are independent of one another, then the observations and a regression line through the observations will align with the 1:1 line on the Z plot. Finally, for a good fitting model, the majority of the data points should lie within the 95% confidence region (calculated using a normal approximation) around the regression line.

A likelihood-ratio test is used here to compare more formally the PP-GPD model without NAO as a covariate to the model with NAO as a covariate in the location parameter. The p-value obtained is less than 2.2×10^{-16}, implying that the inclusion of the NAO is statistically significant (using a 5% significance level) and confirming that the statistical model with a covariate is an improvement upon the basic specification of Part 1.
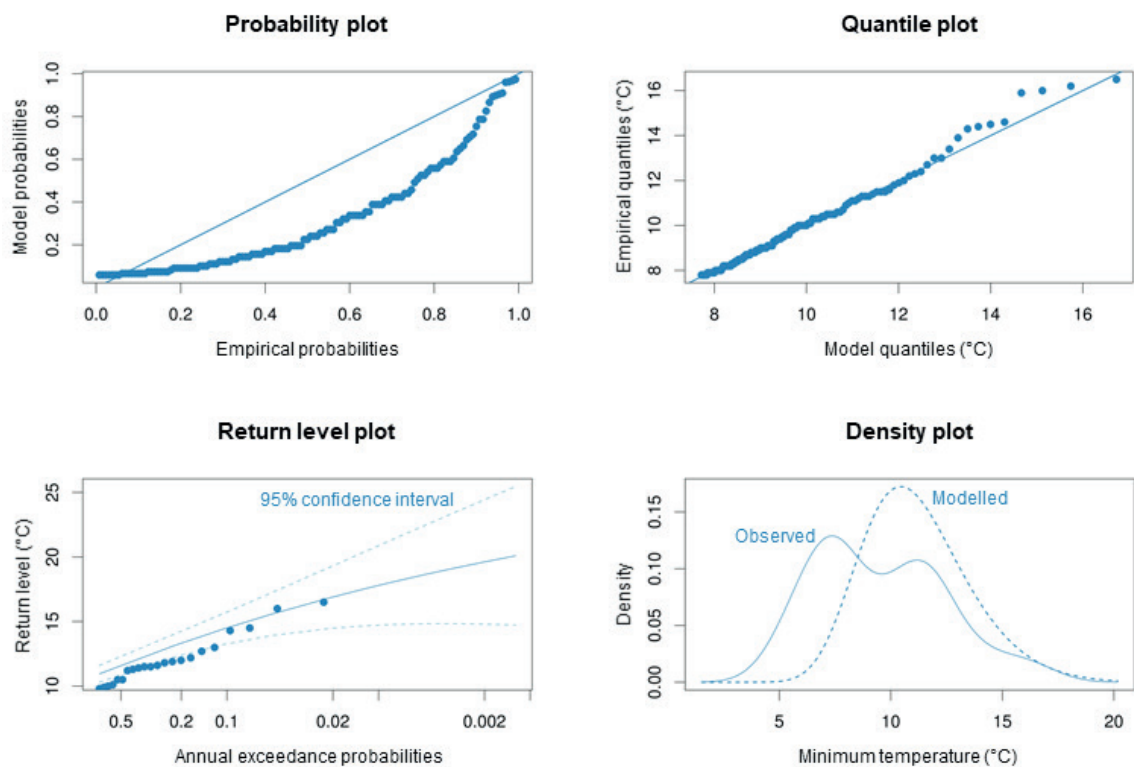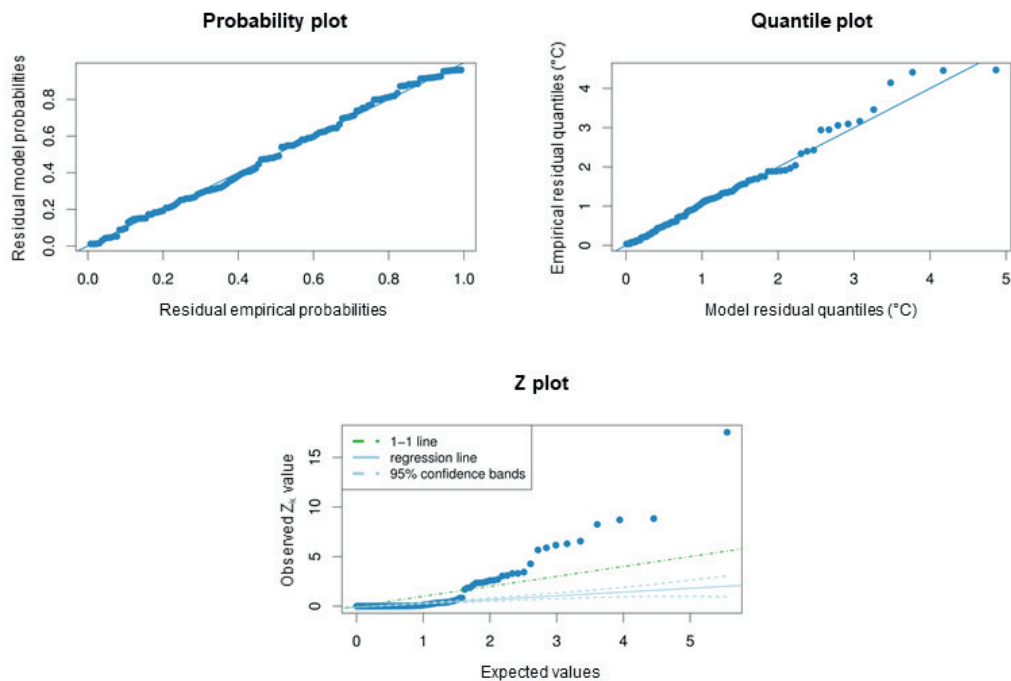

Figure 10. Diagnostic plots of the fit of the PP-GPD distribution to the extreme minimum temperatures at Bala with the NAO index as covariate. The top plots now focus on the fit residuals. The confidence intervals are approximate 95% normal confidence intervals. Note that the minimum temperatures displayed are on a transformed scale (i.e. multiplied by −1).

Case Study 1: Trawsfynydd

Part 3: Removing correlated extreme values

The PP-GPD model has so far assumed that the extreme values selected were independent of one another; an important consideration in any analysis of extreme values (see Section 4 of Volume 2 — Extreme High and Low Air Temperature). In reality, this is not the case. Extreme cold days tend to follow other extreme cold days indicating that the extreme values are indeed autocorrelated (see *Table 4* for an example).

Autocorrelation can be alleviated using a 'declustering' method. This assumes here that consecutive exceedances of the −7.7 °C threshold belong to the same 'cluster' and selects the minimum of the cluster as the single representative extreme minimum temperature for that period. A cluster starts when values go beyond the threshold and ends when they fall below this threshold for a set period of time (a 'run length'). Using the method of *Ferro and Segers (2003)*, the sensitivity of the fit to the run length was examined and a run length of eight days was found suitable for this analysis.

Figure 11 shows the diagnostic plots for the fit of the PP-GPD to the declustered temperatures with the NAO index as a covariate in the location parameter. The probability and quantile plots have not changed appreciably compared to *Figure 10*, and still indicate that the excesses are modelled well by the PP-GPD. However, the Z plot highlights that the Poisson part of the PP-GPD model is much improved: the regression line now aligns with the 1:1 correspondence line and the majority of the points lie within the 95% confidence interval.

The time series plot shows the minimum temperatures (dark blue) along with the effective return levels. Effective return levels are the return levels that would be estimated from the fitted PP-GPD having used the reported daily value of the NAO index. The return levels for AEPs of 0.5, 0.05 and 0.01 (2-year, 20-year and 100-year return periods) are shown in pale blue, pale orange and dark orange respectively. As can be seen from the plot, there is some considerable variability associated with the return levels for each shown return period. This variability is a direct result of the dependency in the PP-GPD model on the NAO index as a covariate.

For a given value of the NAO index, it is possible to derive several AEPs. *Table 7* shows such AEPs conditioned on given values of the NAO index. Note that the NAO index is standardised. The colder extreme minimum temperatures generally occur when the NAO index is large and negative, which is broadly in agreement with meteorological expectations.

However, care should be taken with the interpretation of the temperature return levels in *Table 7*,

as these are the AEPs for specific values of the NAO index and are calculated assuming that the specific NAO index is fixed at a constant value for each day of the year, which is not the case. For example, the daily minimum temperature has a 50% chance of being lower than −13.5 °C in a single year only if the NAO index is −2 for all days in that year.
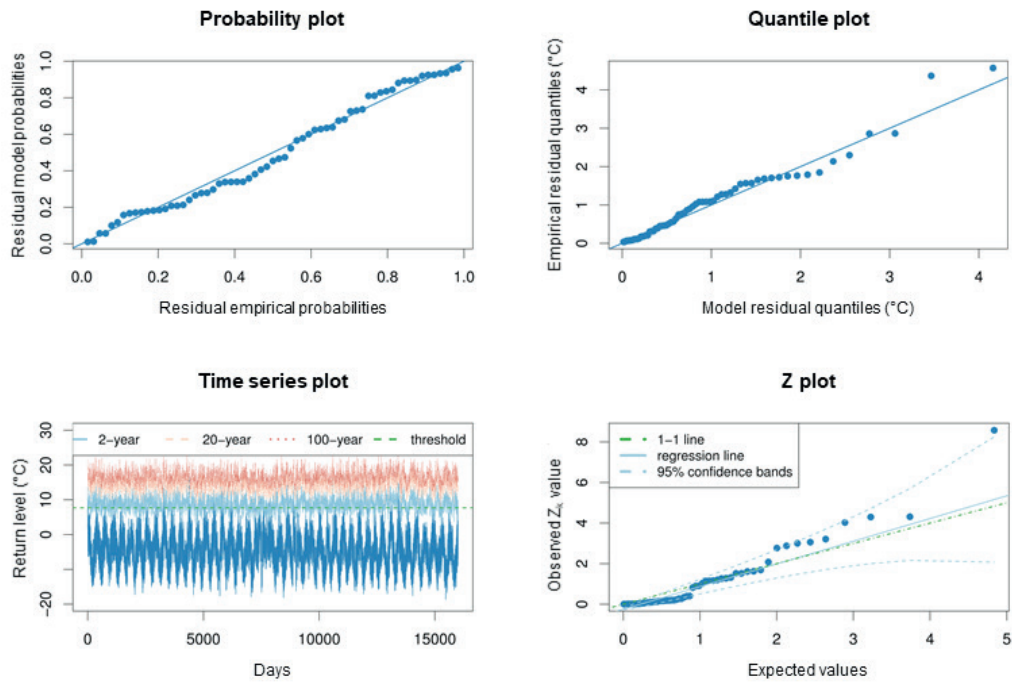
Figure 11. Diagnostic plots of the fit of the PP-GPD distribution to the declustered extreme minimum temperatures at Bala with the NAO index as covariate. The confidence intervals are approximate 95% normal confidence intervals. The top plots now focus on the fit residuals. Note that the minimum temperatures displayed are on a transformed scale (i.e. multiplied by −1).

Table 7. Return levels (°C) associated with particular AEPs, given particular values of the NAO index.

		Standardised NAO index				
		−2	−1	0	1	2
AEP	0.5	−13.5	−11.2	−8.9	−6.7	−4.4
	0.05	−18.7	−16.5	−14.2	−11.9	−9.6
	0.01	−21.3	−19.1	−16.8	−14.0	−12.2

Calculating representative return levels

A more appropriate approach than in Part 3 to obtain a representative AEP would be to calculate the return level associated with the desired AEP for each observation of the NAO index. Taking an average of these return levels would then provide a return level for the specified AEP that is unrelated to the NAO index.

The disadvantage of such an approach is that only observed values of the NAO index are used and they may not be representative of the true NAO index distribution. Alternative approaches are either to fit a statistical distribution to the NAO indices or to estimate the density of their distribution using density estimation techniques such as the kernel density estimation (*Silverman, 1986*). From these fitted distributions, a larger range of NAO indices can then be sampled. Once again, for each value of the sampled NAO index the return levels for the desired AEP can be derived, and an average value of the return level calculated, which is once more independent of the NAO index. One disadvantage of both of these approaches is that, as they are purely statistical, no account is taken of any physical bounds associated with the NAO index.

Table 8 shows the return levels associated with AEPs that are integrated over values of the NAO distribution. The two approaches outlined above were used to derive these return levels. The first approach assumed that the distribution of NAO indices could be modelled using a normal distribution and the second approach sampled the NAO indices from the available data. These approaches give differences of more than 1 °C for an AEP of 0.01. In this particular case diagnostic plots and statistical tests (not shown) in fact suggest that a normal distribution does not fit the NAO indices well and another distribution should be used.

Table 8. Return levels (°C) associated with AEPs independent of the NAO value, calculated following two approaches described in the text.

AEP	Return level assuming the NAO index follows a normal distribution	Return level calculated by sampling the NAO index from the data
0.5	−9.1	−8.8
0.05	−15.3	−14.0
0.01	−18.3	−16.7

Conclusion

The presented characterisation of extreme maximum and minimum air temperatures illustrates the degree of statistical complexity that can be required when fitting statistical models to extreme data, assessing the models, and interpreting the results. In addition, this characterisation only shows one approach within an EVA for analysing extreme data. Other approaches may be more relevant for different extreme datasets, quantifying the uncertainty in the extreme analyses differently, or answering different questions such as how could the probabilities of annual exceedances change during this century as a result of climate change.

Within the research community, current research is starting to focus on more advanced statistical models which can make better use of multiple sources to reduce statistical uncertainty (see Volume 1 — Introduction to the Technical Volumes and Case Studies). These approaches may in the future become standard techniques that can be easily applied.

As a result, the reader may want to consult the latest literature or consider the possibility of engaging experts to benefit from the latest techniques and to ensure the robustness and appropriateness of any statistical analysis to answer their particular questions.

2.2 Seismic, geological and volcanic hazards

Seismic, geological and volcanic hazards are discussed in depth in Volume 7 — Seismic, Volcanic and Geological Hazards. In this section, a description of the seismic hazards at Trawsfynydd and the potential for geological instability is provided, and the probability of volcanic ash deposition is calculated.

2.2.1 Seismic hazards

Impacts

The UK is generally an area of low seismic activity. However, small earthquakes can occur on a regular basis. Seismic design may not be considered for facilities that are classed of low importance by stakeholders, where safety or damage are not critical, or the facilities/contents are not considered sensitive to seismic vibrations. Nevertheless, normal industrial standards are always applicable.

Seismic activity and associated effects translate into:

- earthquakes, when two tectonic plates of the Earth's outer crust displace relative to each other;
- tsunamis, when earthquakes occur under large volumes of water such as oceans or large lakes and set in motion a series of potentially destructive waves;
- liquefaction, when the soil begins to act like a liquid because of losing a substantial proportion of strength and stiffness under the applied force of earthquake vibrations.

The level of shaking experienced during an earthquake is affected by the earthquake magnitude and the amount of energy released, the distance from the earthquake epicentre, and the ground conditions. Earthquakes, tsunamis and liquefaction typically lead to various problems through damage of infrastructure with a potential for injury or death. Furthermore, damage or failure of infrastructure due to earthquake activity may cause other hazards such as fire or flooding (e.g. due to failure of a dam or other water-retaining structure).

Data and history

Trawsfynydd lies in North Wales where earthquakes occur more frequently than other areas of the UK. The British Geological Survey (BGS) provides a historical map of earthquake epicentres for the UK dating back to 1048 AD (see *Figure 12*). From this map, it is evident that North Wales is a more seismically active area compared to other areas of the UK.

Earthquakes with magnitudes ranging from 2.0 up to 3.5 have occurred within a 30 km radius of the Trawsfynydd area. There have been a few cases where several small earthquakes have occurred over small periods of time. In 1941 the area of Bethesda was hit by three earthquakes with magnitudes 2.2, 2.2 and 2.5 in the space of three days (26th September 1941, 27th September 1941 and 29th September 1941 respectively). On 19th July 1984, the largest earthquake in Welsh history (magnitude 5.4) occurred in the Lleyn Peninsula, 50 km from Trawsfynydd, as indicated by *BGS (2018)*.

Studies have indicated that there is little chance of the UK being affected by a tsunami in the future (*Defra, 2005*). Liquefaction is usually observed with saturated, loose sandy deposits, which are not generally present in the Trawsfynydd area. There may however be localised areas where such soils may be present, for example within and adjacent to larger water courses and submerged soils within the Llyn Trawsfynydd area.
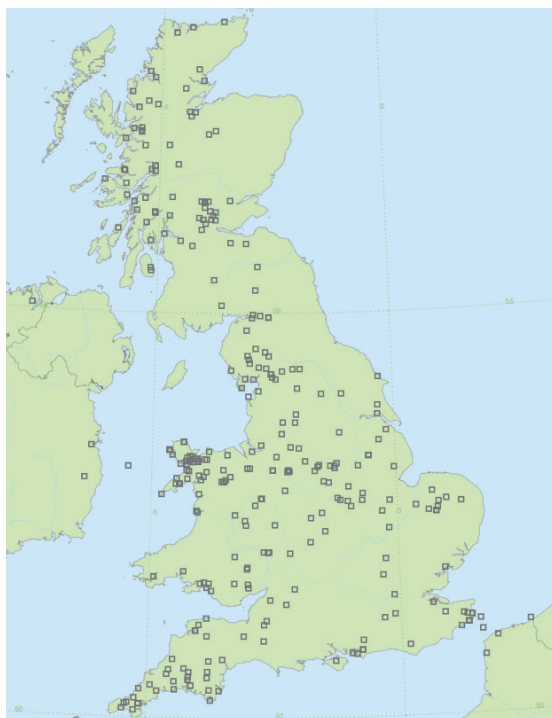

Figure 12. Map showing the location of UK earthquakes since 1048 AD. (UK Historical Earthquake Database, BGS (2018), reproduced with the permission of the British Geological Survey © NERC. All rights reserved.)

Case Study 1: Trawsfynydd

Characterisation

Methodology

As outlined above, North Wales is a relatively seismically active area of the UK. Seismic hazards are typically defined by a single parameter, for example the value of the reference peak ground acceleration (PGA). PGA is the measurement of how much the ground moves during an earthquake; it is measured in metres per second squared (m/s^2) and normally expressed as a coefficient of gravitational acceleration, g (with $g = 9.81$ m/s^2), for example 0.025 g.

Various studies have produced PGA contour maps using different modelling techniques:
- national seismic hazard maps compiled by the BGS for the purposes of seismic zoning within the Eurocode 8 context (*Musson and Sargeant, 2007*);
- community-based seismic hazard model for the Euro-Mediterranean region based on the collaboration of geologists, seismologists and engineers across Europe within the European project 'Seismic Hazard Harmonisation in Europe' (SHARE) (*Giardini et al., 2013*);
- seismic spectra graphs for different site classes from the European Utility Requirements (EUR) for light water reactor nuclear power plants (*Bommer et al., 2011*);
- probabilistic seismic hazard assessments by various authors, e.g. *Goda et al. (2013)*.

Output of these models is discussed hereafter.

Application

PGA estimated using the above sources is summarised in *Table 9*, which highlights the similarity between all values obtained for a no-collapse requirement. The no-collapse requirement is defined in Eurocode 8 as 'the structure shall be designed and constructed to withstand the design seismic action without local or global damage, thus retaining its structural integrity and a residual load-bearing capacity after the seismic events'. *Table 9* does not include EUR values as they are specific to nuclear power plants and not publicly available.

Table 9. Comparison of PGA map output from various sources.

PGA	Return period (no-collapse requirement)		
	475 years	2500 years	10,000 years
Eurocode 8	0.02 to 0.04 g	0.06 to 0.08 g	0.14 g
SHARE	0.04 g	-	0.14 g
Goda et al., (2013)	-	-	0.12 to 0.14 g

Eurocode 8

Following an analysis of the PGA maps in the UK National Annex to Eurocode 8, an average PGA value for the Trawsfynydd area appears to be 0.06 g to 0.08 g for an AEP of 0.0004, i.e. an earthquake with a PGA of 0.06 g to 0.08 g would be expected to occur, on average, once every 2500 years in the Trawsfynydd area (see *Figure 13*).
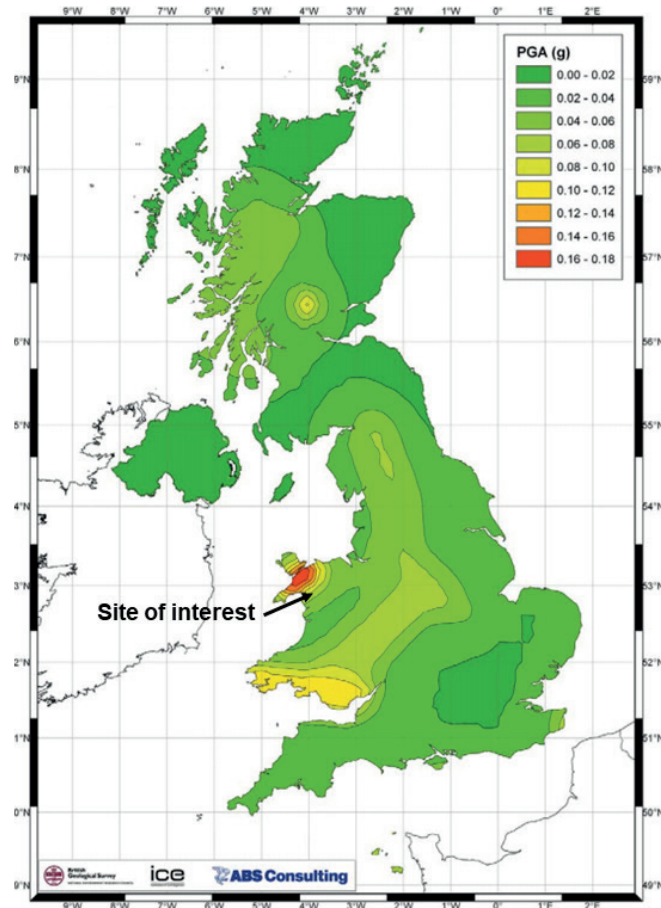
Figure 13. UK PGA values for a 2500-year return period. (Figure 16 of Musson and Sargeant (2007) reproduced with the permission of the British Geological Survey © NERC. All rights reserved.)

To calculate the design PGA, an importance factor should be applied on a project-specific basis. The importance factor in Eurocode 8 is a factor that is used to define the design value of PGA from the reference PGA. Furthermore, the choice of design return period will depend on the significance of the structure and the project-specific standards and requirements.

It should be noted that these maps are not site-specific and are not recommended for sites where previous large magnitude earthquakes have occurred. In this case, the design PGA value should be selected by performing a site-specific hazard analysis. As mentioned earlier, there have been no recorded earthquakes with large magnitude in the immediate area of the site, however this may vary with site selection.

Case Study 1: Trawsfynydd

SHARE

The SHARE seismic hazard map presents the PGA that is expected to be reached, or exceeded, with a 10% probability in 50 years. The Trawsfynydd area appears to be characterised by a PGA value of 0.04 *g*, as shown in *Figure 14*.
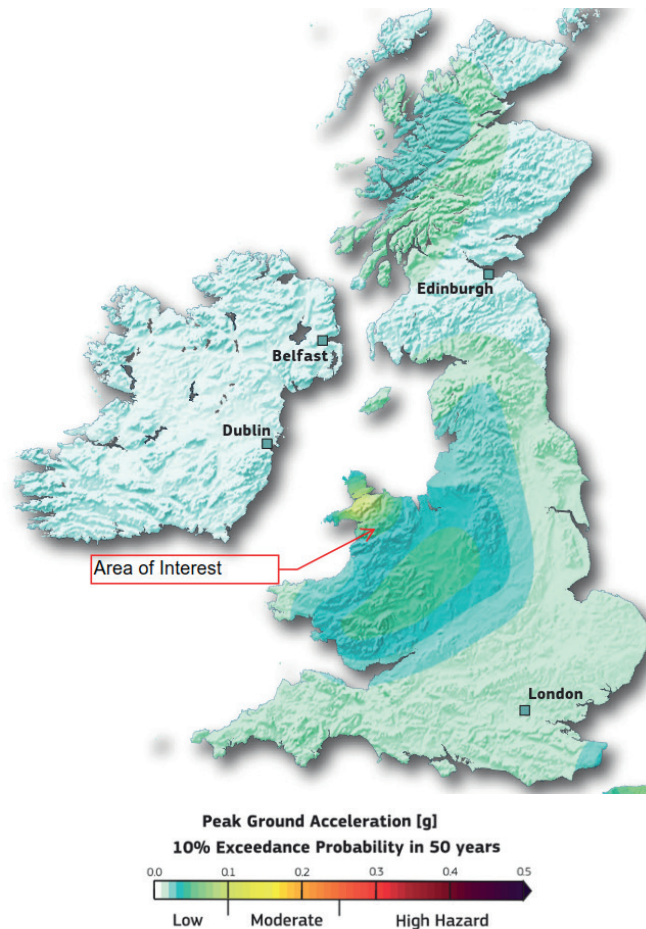
Figure 14. SHARE seismic hazard map for a mean return-period of 475 years considering rock conditions (Giardini et al., 2013).

EUR

EUR uses seismic spectra defined for different site classes. To extract a value of PGA from these graphs, site-specific information such as building frequency and ground type must be considered.

Trawsfynydd could be classed as a hard site (i.e. the ground composition is relatively hard) with a *shear wave* velocity (propagation velocity of seismic shear waves) ranging from 1200 to 2500 metres per second. The EUR requirements are specific to nuclear power plants and the seismic spectra are not publicly available, therefore specific values of PGA are not quoted herein.

Additional study

In 2013, a study was undertaken to compare a conventional source zone model with two seismicity smoothing approaches: *kernel smoothing* and *Geometrical Epicentral Cell*

(*Goda et al., 2013*). The results displayed on each of the maps produced show similar results for the Trawsfynydd area, i.e. the site is characterised by a PGA range of 0.12 g to 0.14 g.

2.2.2 Geological instability

Impacts

Geological instability occurs where there is a loss of ground support and may be the consequence of natural or man-made hazards; it is often termed as subsidence. The character of the potential movements as well as the nature of the infrastructure and its sensitivity to movement is of importance as it will determine the significance of the impact.

Geological instability may be broadly classified within the following categories:
- natural ground instability, e.g. landslides, ground dissolution, soil creep, collapsible ground, running sand/liquefaction;
- natural ground movement, e.g. shrink-swell clays;
- man-made ground instability, e.g. mining, ground water management (shallow compaction, peat oxidation), ground water abstraction, underground construction, oil and gas production.

The incidence and distribution of these hazards within the UK is primarily a function of the underlying geology, but additional factors of influence include topography, weather, and human activities including land use, construction and resource exploitation.

The risks associated with geological instability are for example significant damage to the infrastructure, and associated plant and equipment; loss of serviceability, i.e. resulting in loss of, or reduction in, function; loss of access routes external to the infrastructure site; injury or death; requirement for future mitigation.

Data and history

The phenomena associated with geological instability are recognised as hazards to existing and future development within the UK. A number of organisations, primarily the BGS, have developed data sets to capture the most significant of these; they are available on a number of platforms (see Volume 7 — Seismic, Volcanic and Geological Hazards for more details).

The data records would indicate that in the area of Trawsfynydd there are no records of significant ground instability occurrences from primary hazard sources which include landslides, ground dissolution, shrink-swell clays or underground mining.

However, there may be localised small-scale impacts from other geological instability types, e.g. soil creep on slopes, which are not formally recorded. Mining in the broader area surrounding Trawsfynydd includes an active rock aggregate quarry, former slate quarries and underground mines associated with mineral workings, e.g. gold and lead. These are generally distant from the immediate surrounds of Trawsfynydd, the nearest being the active aggregate quarry on the outskirts of Trawsfynydd village.

Characterisation

The BGS data for landslides record the nearest two historical landslides as events associated with roadside slopes approximately 3 km north of Llyn Trawsfynydd, with a further few approximately 10 km to the south and west, again associated with roads. The majority of the topography and soil conditions immediately surrounding Trawsfynydd is such that there is limited potential for significant landsliding. However, in the wider area the BGS would indicate that there are areas with a moderate potential for landsliding; this being primarily a function of steeper slopes with thicker soil deposits.

The underlying geology is shown in *Figure 2* and comprises bedded turbiditic sandstones, conglomerates and laminated sandstones, and mudstones of Cambrian age. Superficial deposits are absent in many areas, but where present they comprise glacial till (diamicton clay), with localised areas of peat deposits, particularly to the south.

Bedrock geology has no potential for subsidence as a consequence of natural characteristics or mining; although mineral and slate mining is recorded in the wider area, they are remote from the immediate site locality. Clay deposits occur in proximity, but they are of a mineralogy that is not susceptible to changes in moisture content and therefore not prone to significant shrink-swell.

There are areas of surface peat deposits, most extensively on flatter ground to the south. Peat is a weak and highly compressible organic deposit generally unsuitable below foundations or earthworks. Where it is present on sloping ground, peat has the potential for instability caused by natural triggers such as rainfall events or anthropogenic influence (e.g. construction activity disturbance). Civil design would need to address these aspects if developments occur in such localities.

2.2.3   Volcanic ash deposition

Impacts

Volcanoes are a source of a number of hazards, with ash being the most frequent and having the widest impact. Ash falls generally do not threaten human life directly, but even low

atmospheric concentrations and deposition of only a few millimetres impact public health and can create disruption to infrastructure services, most notably aviation (*Jenkins et al. (2015)*; see also Section 2 of Volume 7 — Seismic, Volcanic and Geological Hazards). Example impacts include clogging of air and water intakes, handling and filtration systems; adverse impacts upon mechanical and electrical plants, including water treatment plants; flash-over of power lines and transformers; impact upon external communication equipment; obscuring of road markings; increased corrosion to components; and respiratory health impact.

The incidence and distribution of these hazards within the UK is subject to the occurrence of a volcanic event within relative global proximity of sufficient explosivity to generate large volumes of fine ash projected into the upper atmosphere, together with a sustained weather pattern providing the transport of suspended ash over the UK.

Data and history
The UK is no longer volcanic and does not have a credible risk of future volcanism, but there are localities regionally which are active and significant to the UK, primarily the Icelandic volcanoes.

Ash deposition has historically occurred over the UK, with traces of ash deposition found within soil deposits principally in Scotland; these being dated within the last 10,000 years. More recent Icelandic volcanic eruptions, the Laki and Grímsvötn from 1783 to 1785, Eyjafjallajökull in 2010 and Grímsvötn in 2011 adversely impacted the UK. The Laki eruption produced fine ash and sulphuric acid aerosol, known as the 'Laki Haze', which affected the northern hemisphere for months. The ash from the 2010 and 2011 events had an adverse impact upon aviation.

A serious focus upon modelling and prediction of ash levels over the UK followed the Eyjafjallajökull 2010 eruption which grounded aviation for eight days. The ash from this eruption had no other impacts on the UK.

Volcanic events are monitored at both national and global levels with collaboration between organisations. There are nine Volcanic Ash Advisory Centres (VAAC) worldwide; these are International Civil Aviation Organization (ICAO) designated centres responsible for issuing advisories for volcanic eruptions. The London VAAC is hosted and run by the Met Office and has responsibility for issuing advisories from volcanic eruptions originating in the north-eastern corner of the North Atlantic which includes Iceland and Jan Mayen (a volcanic island belonging to Norway). Information on the status of volcanoes and signs of unrest or activity is provided

to the VAACs by the State Volcano Observatory, which for Icelandic volcanoes in the London VAAC region is the Icelandic Meteorological Office.

Standard advisories issued by London VAAC are the Volcanic Ash Advisory (VAA) and Volcanic Ash Graphic (VAG) for three flight levels. Supplementary guidance products are provided by the Met Office under designation from the UK Civil Aviation Authority (CAA) in the form of charts showing ash concentrations in the volcanic cloud. Advisories and charts are issued on a six-hourly basis during a volcanic eruption, providing guidance up to 18 hours ahead for the VAA/VAG and up to five days ahead for the CAA. The volcanic ash forecasts are provided to the standards and tolerances set by the regulator, and support decision-making by the CAA as the lead agency, National Air Traffic Services (NATS) and airlines.

Characterisation
Methodology
The probability of a significant ash event is dependent on a number of factors, including the occurrence of an explosive volcanic event of sufficient magnitude, duration and type to eject fine ash materials high into the atmosphere, coupled with weather conditions that will transport ash a sufficient distance and in such concentrations to impact sensitive receptors.

The VAAC reactive modelling does not provide the probability of future significant ash fall. However, a volcanic ash hazard assessment for EDF Energy nuclear power station sites was recently carried out by the *University of Bristol (2016)* with project funding from the Natural Environment Research Council (NERC). It included the identification of volcanic sources capable of producing ash that reaches the UK; the development of frequency-magnitude relationships for each source; an analysis of the range of meteorological conditions and their probability of occurrence; three-dimensional dynamic ash transport modelling; and post-processing to evaluate the volcanic ash hazard at sites of interest in the UK. This study is used here to estimate the probability of volcanic ash deposition at Trawsfynydd.

Application
Modelling by the *University of Bristol, (2016)* has derived that the exceedance of ground level ash concentration of 500 micrograms per cubic metre ($\mu g/m^3$) within the UK has an annual probability of about 1 in 300, with the duration of ash fall between 20 and 45 hours.

The study concluded that, for the UK (including Trawsfynydd), the vast majority of ash particles will be smaller than 10 micrometres (the respirable range, termed PM_{10}), and the most likely

source is a moderate-size Icelandic eruption. This ground-level ash concentration will potentially impact filtration systems on a wide range of infrastructure, and human health (daily limit for good air quality is 50 µg/m³ not to be exceeded more than 35 days in a year, as transposed into UK legislation by the Air Quality Standards Regulations 2010 (*HM Government, 2010*)) leading to increased maintenance and possible workforce disruption. Higher ash concentrations (1 in 1000 annual probability) may disrupt air transportation and affect supply chains. At the 1 in 10,000 annual probability of occurrence, ash thicknesses are still approximately two orders of magnitude smaller than those required to cause ground transportation issues. The impacts on water supplies and telecommunications are uncertain.

The confidence levels for these predictions are subject to assumptions regarding the frequency of suitable volcanic events and weather patterns, as well as the ability to model the movement of the ash; there remain some major uncertainties with respect to the prediction of volcanic events, particularly ash-producing moderate events. The prediction of volcanic ash remains a subject of ongoing analysis (*Chai et al., 2017*; *Loughlin et al., 2015*; *Zidikheri et al., 2017*).

2.3   Natural hazard combinations

Elsewhere in the guidelines and the case studies, the various hazards discussed are largely considered in isolation. However, especially in relation to certain severe weather events, it is possible for more than one natural hazard to occur simultaneously, or for one hazard to occur soon after another and so enhance the impacts of an existing situation.

Research undertaken during this project identified thirty-two natural hazards of relevance to the energy infrastructure (see Volume 12 — Hazard Combinations), such as natural hazards of meteorological origins, marine origins, biological origins, etc. Not all combinations of these hazards are plausible, either for physical reasons or because they are not relevant to the location of interest.

The screening of hazard combinations and an example of in-depth characterisation of one selected combination (high temperatures and low summer rainfall) are discussed here.

2.3.1   Impacts

Combinations of meteorological natural hazards have been seen in recent history. On 17th January 2013, strong winds and heavy snowfall forced the closure of many schools in Wales. Storm Brian struck the UK on 21st October 2017 (*Met Office, 2017a*); very strong winds coincided with high tides resulting in flooding of coastal areas in Wales and other parts of the

UK. Trains and ferries were cancelled and seafront roads closed because of the weather. Fallen trees and other debris on railway tracks caused cancellations and disruption on some lines. Hail and rain often occur together or in quick succession; hail from a storm would be followed by rain as the storm moves over a fixed point. Flooding from heavy rainfall can be exacerbated by hail; the hail can block drains and channels, causing or enhancing flooding, as happened in Ludlow in June 1982 (*Meaden, 1982*) and Ottery St Mary in October 2008 (*Clark, 2011*).

Flooding as a consequence of extreme rainfall is the main peril that has affected energy infrastructure in recent years. During December 2015, 20,000 homes in Rochdale near Manchester were left without power following torrential rain that flooded a substation. On 29th and 30th December 2015, Storm Frank, an unusually deep area of low pressure, produced heavy rain and strong winds across the UK (*Met Office, 2016*). Thousands of homes in Northern Ireland and Scotland were left without power. In the village of Ballater, Aberdeenshire, electricity poles and conductors were washed away by the rising flood waters.

From historical records correlated by the BGS and numerous worldwide researchers, it has been established that there is a strong correlation between the frequency of occurrence of landslides and extreme rainfall events. The stability of soils and bedrock on sloping ground is a balance between the disturbing force of gravity and the resistance to movement by the properties of the ground, primarily its 'strength'. Groundwater and the consequent hydraulic pressure, both positive and negative, have an impact upon strength properties and can – where rainfall intensity-duration thresholds are exceeded – lead to landslides, the scale and impact of which will be variable. Roadside historical landslides in the vicinity (see *Section 2.2.2*) may have occurred due to one or more rainfall event (but this is not recorded).

Similarly, seismic events introduce a disturbing force which can destabilise currently stable slopes. The seismicity of Trawsfynydd is of a relatively low magnitude (see *Section 2.2.1*) and is not expected to initiate landslides. It should however be considered where developments are of significant sensitivity and/or the required design AEP is particularly low, resulting in the need to adopt a higher ground acceleration factor. The potential for liquefaction requires the presence of groundwater and the presence of soils of a characteristic that are susceptible to liquefaction, typified by loose silt/sands. Although most of the soils of a general locality may not be of this type and therefore not susceptible to this phenomenon, there may be localised areas where such soils may be present, for example within and adjacent to larger watercourses and submerged soils.

As the above examples show, the relationship between the occurrence of a particular hazard

Case Study 1: Trawsfynydd

combination and the occurrence of a particular impact (or impacts) is highly complex, and dependent on more than just the hazards in question. In this document and the corresponding guideline, the characterisation focuses solely on the combination of hazards. It is assumed that the reader will have some level of understanding about why a particular hazard combination is relevant for their purpose, which in turn is likely to stem from a recognition of the possible impact of that hazard combination on the energy infrastructure of interest.

2.3.2   Screening out hazard combinations

Many combinations of hazards can be screened out for Trawsfynydd. Generally, the screening consists of identifying hazard combinations in two steps:

1. Eliminating those combinations which are unphysical or irrelevant;
2. Identifying hazard combinations which have occurred or could occur in order to characterise them further.

Some hazard combinations are unphysical anywhere, which applies particularly to those involving a meteorological event. Meteorological observations indicate that many hazards could not occur together at the same location because they are created by very different conditions or at very different times of year. Examples of unphysical hazard combinations are:

- extreme high air temperatures would not occur simultaneously with extreme low air temperatures;
- snowfall and high temperature clearly could not occur together;
- extreme high groundwater levels would not coincide with a drought;
- fog could not occur with high winds.

Some hazard combinations (involving hazards related to the marine environment, such as large swell, waves and sea levels) are not relevant at Trawsfynydd because the site is inland. Waves and swell are not likely to be an issue at Llyn Trawsfynydd, given that the lake is quite shallow and the longest fetch (the distance that the wind has blown over the water) is only about 5 km. The maximum possible wave height can be estimated using a manual wave forecasting diagram (*Burroughs, 1998*). If very strong winds (30 m/s) were orientated with the longest axis of the lake, the small fetch of the lake means the largest waves produced would be about 2 m high, which would be unlikely to have a severe impact.

The remaining hazard combinations can be considered possible for Trawsfynydd. Some combinations may have occurred, others carry a low probability of occurrence, while others still may include at least one hazard that is not predictable.

Case Study 1: Trawsfynydd

The characterisation of the remaining hazard combinations is contingent on several considerations. For example:

- How critical are the possible impacts to the infrastructure?
- Are there data to characterise the hazard combination?
- Is it possible to conduct a quantitative assessment? For example, any hazard combinations involving a meteorite impact or space weather event could, in principle, occur anywhere and at any time, making it difficult or impossible to conduct a quantitative assessment of such a combination.
- Is one hazard possible but not predictable? One approach for the unpredictable hazard is to take a pre-defined scenario of occurrence for that hazard (where this exists), and consider the implications of that scenario for the energy infrastructure in question. Depending on the nature of the other hazard in the combination, it may be possible to conduct a more quantitative analysis for that other hazard.

For simplicity, in this case study, the next sections explore data availability for a chosen hazard combination, namely low summer rainfall and high temperatures, and illustrate one way to characterise this combination in depth. The reader should note that in a real assessment, there may be a need to characterise multiple combinations, even if they are considered to be of low probability, because low-probability hazards can often yield a major impact (hence their frequent appearance in some regulatory frameworks).

2.3.3 Data

Coincident observations of many hazards either do not exist or need to be created from different data sources. The reader is referred to Volume 12 — Hazard Combinations for a list of relevant data sets for natural hazards in the UK, as well as to the individual guidelines relevant for the natural hazards considered.

Changes in the occurrence and magnitude of many individual hazards have been examined using observations and climate models, but very few studies have considered two hazards at the same time. For instance, there are many studies of climate change impacts on heavy and extreme rainfall, but very few consider the combined risk of heavy rain and strong winds. Consequently, changes in many of the joint hazards under a warming climate need to be inferred from separate studies. The co-occurrence of low summer rainfall and high temperatures is characterised in further depth in *Section 2.3.4.*

Trawsfynydd weather station operated between 1961 and 1998 (see *Section 1* for information on

the location). Measurements of temperature were available from 1961 to 1995, and from 1967 to 1983 for rainfall, thereby providing too short a record for the purpose of this analysis. There are various ways of extending a weather record at a given location. One is the use of a nearby weather station with a longer record available (e.g. Bala weather station, as demonstrated in *Section 2.1*). For illustrative purposes, another method is used here. Time series of mean daily maximum temperatures and total rainfall, each over the summer periods (June, July, August), were extracted from the nearest point in a 5 km daily gridded data set created from UK weather stations and spanning the period of 1961 to 2016 (*Perry and Hollis, 2005*; *Perry et al., 2009*). The resulting time series of annual values are shown in *Figure 15*. Note that better statistics could potentially be gained by pooling data from neighbouring grid points; assuming these grid points were not dramatically different from the grid point nearest to the site (e.g. in altitude or exposure), the rainfall at the site could, in theory, just as easily have fallen at surrounding locations.

2.3.4   Characterisation

A common methodology for assessing a combination of two hazards is the calculation of their joint probability using a *copula* (see Volume 12 — Hazard Combinations). Previous studies have calculated the joint probabilities of low summer rainfall coinciding with high temperatures in different parts of the world (*AghaKouchak et al., 2014*). This calculation is demonstrated at Trawsfynydd for high temperature and low rainfall, as an illustrative combination.

Methodology

There are several methods available for calculating joint probabilities of extreme events, including the joint tail approach (*Ledford and Tawn, 1997*) and the conditional extremes approach (*Heffernan and Tawn, 2004*). Here, a copula function is used to calculate the joint probability. Copulas are functions used to describe the dependence between random variables. They have been used widely in finance and in hydrology, as well as to assess the joint probability of droughts accompanied by high temperatures.

Briefly, any joint distribution can be written in terms of distribution functions for a single variable and a copula, which describes the dependence structure between the variables. Functions to fit copulas to data are readily available in the R programming language (*R Core Team, 2013*). The calculation consists of four steps:

1. Assessment of possible dependence;
2. Transformation of the data to the [0, 1] range;
3. Choice and fitting of a copula;
4. Calculation of joint probabilities.

Application

Step 1: Assessing possible dependence between high temperatures and low rainfall

The first step is to compare the two datasets and establish whether there is any evidence for a dependence between them as well as the nature of the dependence. The mean summer maximum temperatures and summer total rainfall amounts for each year are shown in *Figure 15*. Values for the whole summer are used, rather than daily values, because the examination of high temperature and low rainfall pertains to the potential for drought, which is a phenomenon that requires some persistence of conditions over time. The rainfall data are plotted against the temperature data in the same figure.

There is a suggestion of a weak dependence between the two datasets, mostly for high temperatures and low rainfall (< 150 mm). This correlation is weak and negative (high temperatures occur with low rainfall).

Some copulas are only suitable for analysing positively correlated data. Hence, for this example, the temperature data are adjusted by subtracting them from 23 °C (the highest temperatures lie between 22 °C and 23 °C). By doing so, higher temperatures are adjusted into small values and lower temperatures into large values. The summer rainfall totals are shown as a function of these adjusted temperatures in *Figure 15*. A weak positive correlation is now apparent when both variables have small values.

Any dependence between two variables in the scatter plots of *Figure 15* can be hard to identify. Another useful tool for quickly assessing dependence (or independence) between two variables is the Kendall plot, or K-plot (*Genest and Boies, 2003*). The K-plot is based around ranked statistics of the dataset. For each pair of values, the number of remaining pairs with smaller values is counted, and the counts are then ranked. Data that have a degree of dependence will have higher numbers of points less than any chosen pair than pairs of points which are completely independent (assuming a positive correlation). The amount of curvature in the graph is characteristic of the degree of dependence in the data. Different degrees of dependence between two variables are illustrated on a sample K-plot in *Figure 16* (left). Variables that are independent lie along the leading diagonal (shown by the black crosses). Partial or perfect dependence is shown by the coloured lines for variables that are positively and negatively correlated. Positively correlated variables lie above the diagonal, and negatively correlated variables lie below the diagonal.

A K-plot for the rainfall and temperature data is shown in *Figure 16* (right). The data points lie between the leading diagonal and the curved dotted line, indicating a partial positive dependence between the temperatures and rainfall, as was already inferred from the scatter plots of *Figure 15*.
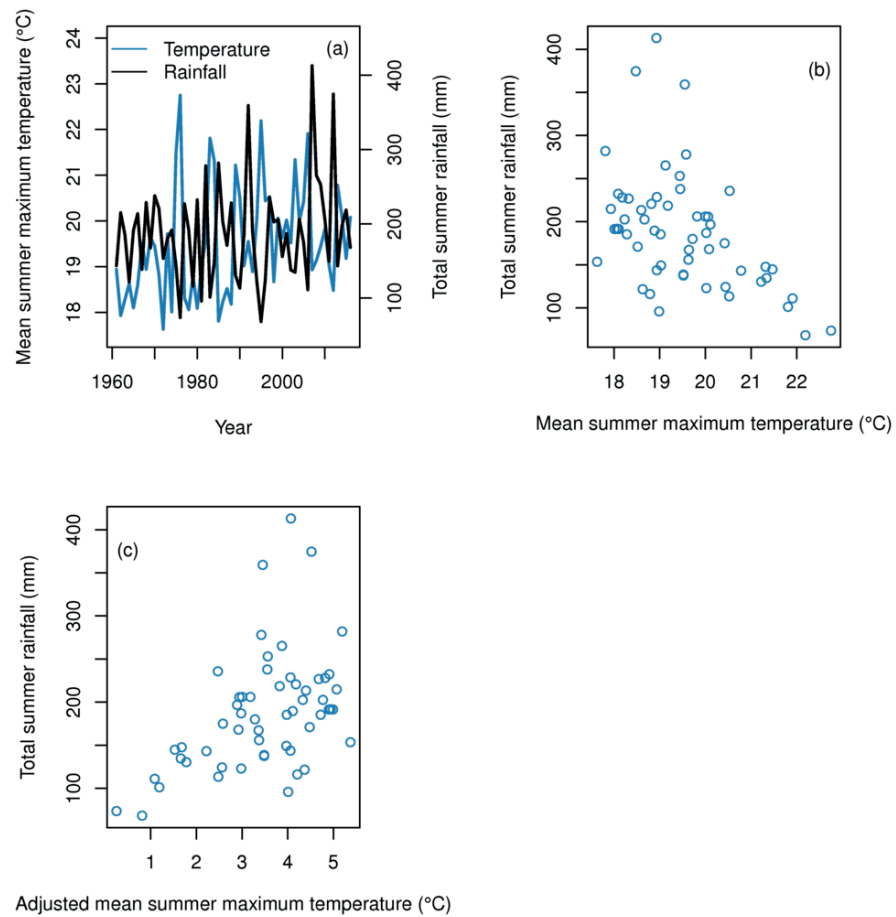

Figure 15. (a) Time series of mean summer maximum temperatures (blue) and summer total rainfall (black). (b) Summer rainfall as a function of summer temperature. (c) Summer rainfall as a function of adjusted temperatures.
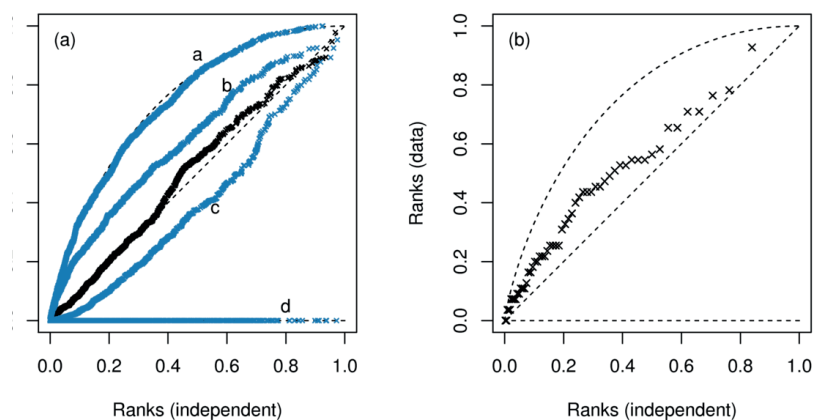
Figure 16. (a) Example of K-plot, showing the appearance of two datasets with no dependence (black line on leading diagonal), perfect positive dependence (curve a), partial positive dependence (curve b), partial negative dependence (curve c), perfect negative dependence (curve d). (b) K-plot for summer rainfall and adjusted temperatures at Trawsfynydd. Note that the ranks have been normalised to the range [0, 1] by dividing by the number of data points.

Case Study 1: Trawsfynydd

Step 2: Transformation of the data to the [0, 1] range

Before fitting a copula, the data have to be transformed onto the [0, 1] range. A function is fitted to each of the two datasets, which describes their distributions. In the context of copulas, this function is called the *marginal distribution function*. A marginal distribution function describes the probability distribution of a single variable. Several functions were fitted to the temperature and rainfall data and the function with the best fit was selected based on *Akaike information criteria* (AIC) and other goodness-of-fit statistics.

For the data used here, a Weibull function was the best fit to the temperature data (*Figure 17*) and a gamma function for the rainfall data (*Figure 18*). The fit of these functions to the data is shown in the upper left panels. The corresponding *cumulative distribution functions* (CDFs), which were used to transform the data to the range [0, 1], are shown in the upper right panels of each figure. The empirical CDF (solid circles) is derived from the data, and the theoretical CDF (smooth line) is calculated from the fitted function.

Also shown in the lower panels of *Figure 17* and *Figure 18* are the corresponding quantile and probability plots. The quantile plot compares the distributions of the original data and the fitted function, and magnifies deviations between them in the tails. The probability plot illustrates how well a theoretical distribution fits the given data (i.e. the observed distribution), and magnifies deviations in the middle of the distribution. If the fit of the functions to the data was near-perfect, all the points would lie along the leading diagonal.
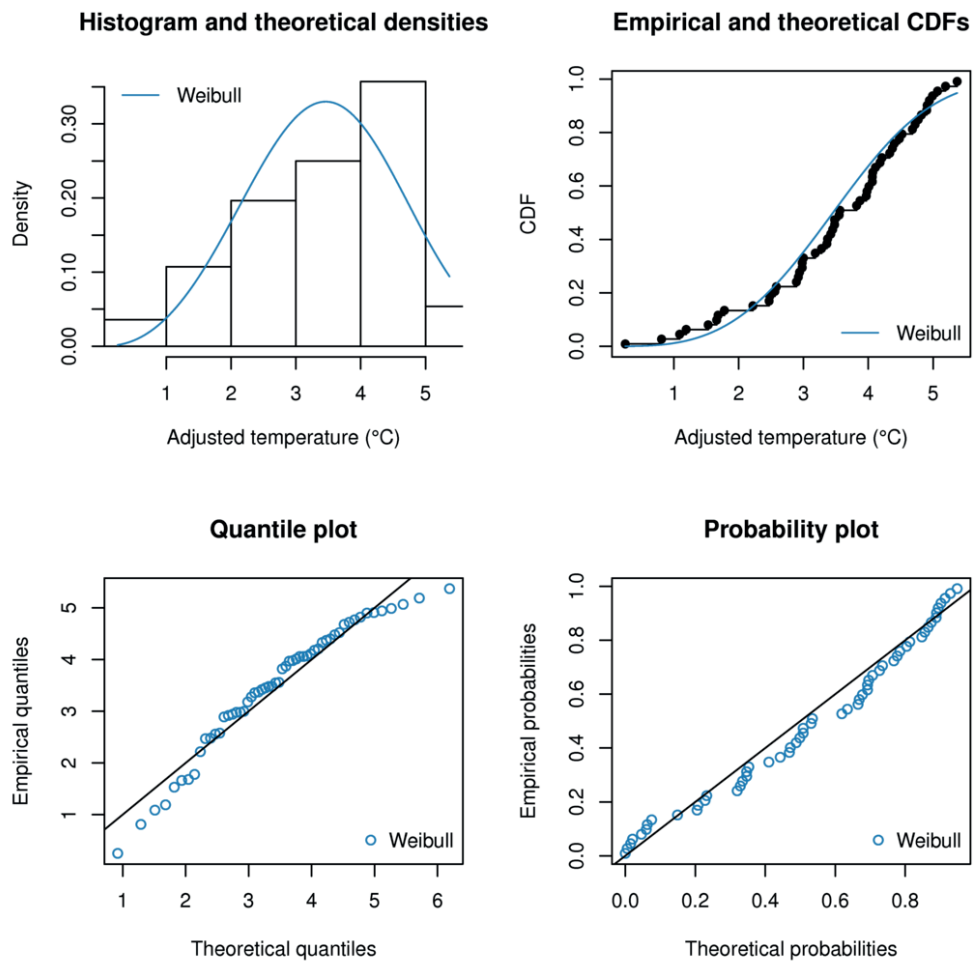
Figure 17. Fitting of a Weibull distribution to the transformed temperature data. The distributions of the data and fitted function (densities) are shown in the top left panel. The empirical (derived from the data) and theoretical (from the fitted Weibull function) cumulative distribution functions are shown in the upper right panel. The quantile plot (lower left panel) compares the quantiles of the data distribution with those of the Weibull function. The probability plot (lower right panel) compares the empirical cumulative distribution function of the data with the cumulative distribution function from the Weibull distribution. The quantile plot highlights differences in the tails of the distributions, whereas the probability plot highlights differences in the centres of the distributions.
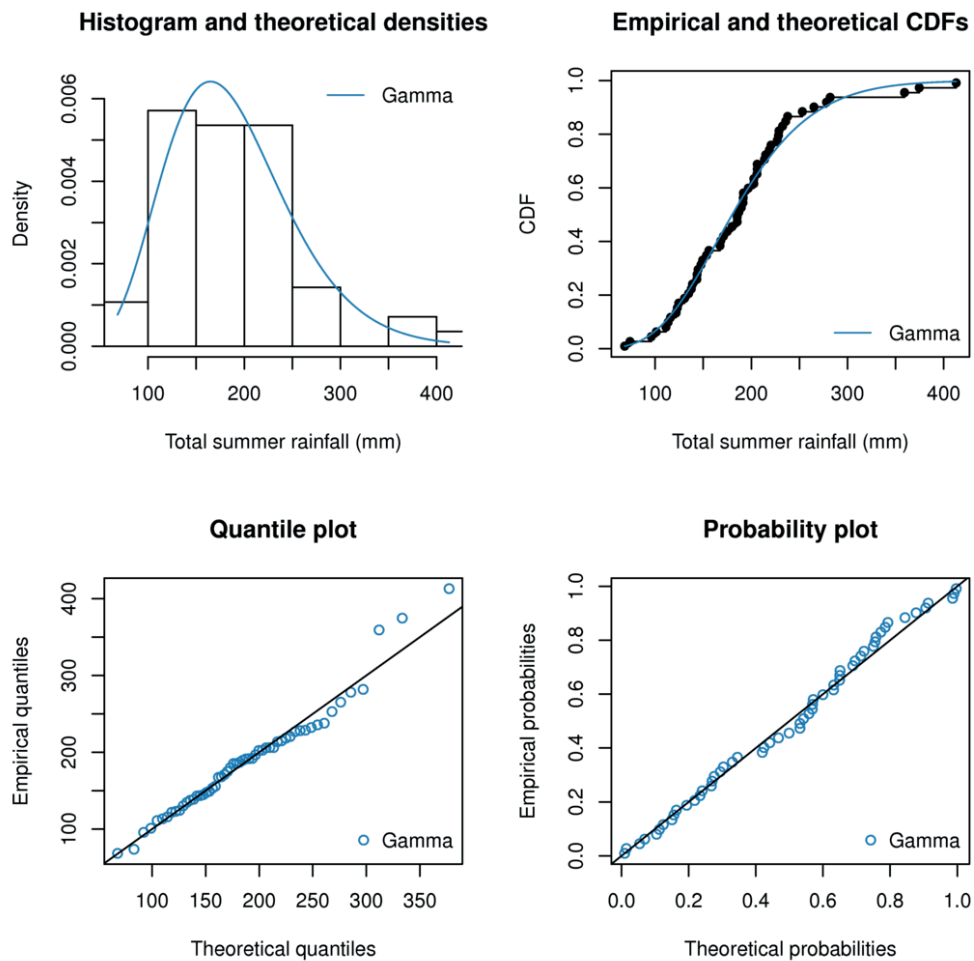
Figure 18. Fitting of a gamma distribution to the rainfall data. The distributions of the data and fitted gamma function (densities) are shown in the top left panel. The empirical (derived from the data) and theoretical (from the fitted gamma function) cumulative distribution functions are shown in the upper right panel. The quantile plot (lower left panel) compares the quantiles of the data distribution with those of the gamma function. The probability plot (lower right panel) compares the empirical cumulative distribution function of the data with the cumulative distribution function from the gamma distribution. The quantile plot highlights differences in the tails of the distributions, whereas the probability plot highlights differences in the centres of the distributions.

In *Figure 17*, the probability plot shows that the Weibull function reproduces the middle of the distribution reasonably well, but the quantile plot indicates that the tails of the distribution are not captured very well. In *Figure 18*, all four panels indicate that the gamma function fits the data reasonably well, except for the very largest rainfall values which are underestimated. Better fits to the distributions could possibly be found if other functions were tested.

Step 3: Choosing and fitting a copula
Now the marginal distributions are known, the next step consists of choosing a copula to represent the dependence between the two variables.

There are many different copula functions which represent various types of dependence between two datasets – weak or strong dependence, dependence for only very large or very small values, or dependence for extremes of both variables (*Dupuis, 2007*). The data shown in *Figure 15* and *Figure 16* indicate dependence when both variables have low values, but no dependence at higher values. The Clayton copula is suitable for this type of dependence. Ideally, several different copulas would be selected and the best one chosen based on goodness-of-fit statistics (see *Genest et al. (2009)* for a review of suitable methods, and *Requena et al. (2013)* for a practical example).

The Clayton copula was fitted to the data after transformation to the range [0, 1] using the marginal distributions identified in the previous step. Next, 1000 random values were generated from the fitted Clayton copula, which are in the range [0, 1]. These random values are transformed back to the original data (i.e. actual values of temperature and rainfall) using the inverses of the CDFs shown in *Figure 17* and *Figure 18*.

A scatter plot of the 1000 values generated from the Clayton copula and the observed data is shown in *Figure 19*. The simulated values have a similar pattern to the observed data, suggesting the Clayton copula was a reasonable choice. Some of the simulated values lie outside of the range of the observed data. Correlations (based on *Kendall's tau*) in the original and simulated data are 0.34 and 0.27 respectively. These values indicate weak correlation, as before (a value of 1 for Kendall's tau indicates a perfect correlation and a value of 0 indicates none); they are in reasonable agreement, but ideally, the two correlations would be closer in value.
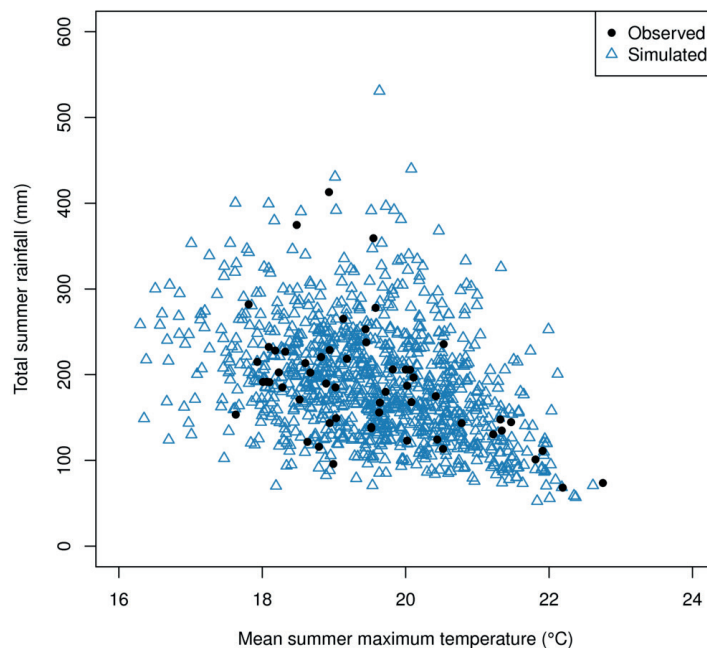

Figure 19. Scatter plot of observed data (solid circles) and simulated data (open triangles) using the Clayton copula.

Case Study 1: Trawsfynydd

Step 4: Calculating joint probabilities

The joint probability of an event can now be calculated using the fitted copula. For this example, the probability of mean summer maximum temperatures exceeding 22 °C and summer rainfall being below 100 mm at Trawsfynydd is calculated; the values correspond to very warm and dry conditions. As the temperature data were transformed by subtracting them from 23 °C, so the calculation uses the condition that the transformed temperature is less than or equal to 1 °C. First, a large number of random samples (e.g. 100,000) are generated using the fitted copula and transformed back to actual data values. Next, the joint probability is calculated as the number of randomly generated points for which the temperature is less than 1 °C and the rainfall is less than 100 mm, divided by the total number of points generated. For the condition used here, the number of points is 869. The uncertainty in this result can be estimated assuming the numbers of points meeting the criteria above follow a Poisson distribution. The uncertainty is the square root of the number of points, which is 30 in this example. Hence, the probability and its uncertainty is 0.00869 ± 0.00030.

The return period is the inverse of the probability, which for this example is 115 ± 4 years. An alternative method would be to generate multiple samples of 100,000 points (e.g. 20,000 times), count the number of points that exceed the two thresholds in each sample, and then calculate the mean and standard deviation of the 20,000 estimates. This latter approach gave a return period of 117 ± 4 years, in very good agreement with the previous estimate.

Looking at the original observed data (*Figure 15*), there are in fact two data points which fulfil the joint criteria above. In a data series spanning approximately 50 years, an approximate return period could be inferred of 25 years. The method described above effectively 'fills in' the dataset with many more points (as represented in *Figure 19*), and allows a return period to be estimated – based on this larger pseudo-dataset – that is longer than that based on the observed data alone. This suggests that the two observed points are actually quite unusual despite their having occurred within the same ~50-year period. The difference between the return periods estimated in these different ways indicates one of the potential pitfalls of basing such a calculation solely on observed data.

3. Conclusions

This document provides an example of how the guidance for the characterisation of three families of natural hazards, namely extreme temperatures, seismic/geological/volcanic hazards and hazard combinations, could be applied to the site of Trawsfynydd in North Wales. It also constitutes an example of how the guidance could be used to characterise the natural hazard risk at inland sites elsewhere in the UK.

The assessment of extreme temperatures has encompassed maximum and minimum air temperatures, rapid changes in air temperature, extreme water temperatures, frazil ice, and wildfires. The analysis of extreme air temperatures has been described in detail for this case study.

The study of extreme air temperatures has been based on observed daily minimum and maximum air temperatures recorded at a nearby weather station (used because of its slightly longer data record than that at the Trawsfynydd site). An extreme value distribution was fitted to both the maximum and minimum air temperature data and return levels were estimated for annual exceedance probabilities of 0.5, 0.05 and 0.01. Two distinct extreme value distributions were fitted, a generalised extreme value distribution and a Poisson generalised Pareto distribution, to illustrate two standard approaches for extreme value analyses. The illustrative extreme value analysis indicated that maximum (minimum) air temperatures of 27 °C, 32 °C and 35 °C (−9 °C, −14 °C to −15 °C and −17 °C to −18 °C) are expected to be exceeded annually with a probability of 0.5, 0.05 and 0.01 respectively. To place this analysis in some context, the hottest and coldest daily temperatures ever recorded at Trawsfynydd itself were 32 °C (2nd August 1990) and −11 °C (19th November 1962).

The illustrative extreme value analysis has assumed that the data contain no long-term trend due to climate change. However, the climatologies of maximum and minimum temperatures suggest otherwise. UK average temperatures vary considerably from year to year; calculating linear temperature trends over the period 1914 to 2006, all regions of the UK have become warmer, with annual average daily maximum, mean, and minimum temperatures all increasing (*Jenkins et al., 2008*). Almost all of these observed regional trends are statistically significant.

The numbers and frequencies of heatwaves are projected to increase across the UK as the climate warms, and the number and intensity of cold days to decrease (*IPCC, 2013*; *Murphy et al., 2009*). *Sanderson and Ford (2016)* estimated an increase in the number of UK heatwave days by up to two days per decade during the twenty-first century.

Weather conditions for severe wildfires already occur under the present climate. Climate change in the UK is projected to increase the risk through drier summers and possible changes in the frequency and intensity of droughts (*Brown et al., 2016*).

The assessment of seismic, geological and volcanic hazards has encompassed earthquakes, tsunamis, liquefaction, landslides, shrink-swell clays, ground instability from mining, and volcanic ash deposition.

Although the UK experiences relatively low seismicity, earthquakes occur more frequently in North Wales than other areas of the UK. National seismic hazard maps have been used to calculate the peak ground acceleration for various return periods. Peak ground accelerations of 0.02 to 0.04 *g*, 0.06 to 0.08 *g* and 0.12 to 0.14 *g* have been associated with return periods of 475, 2500 and 10,000 years respectively. Tsunamis and liquefaction pose no threat to the site. No potential was found for landslides or subsidence at Trawsfynydd, but in the wider area the British Geological Survey would indicate that there are areas with a moderate potential for landsliding. The area's clays were not of a characteristic prone to significant shrink-swell. The risk of volcanic ash deposition at Trawsfynydd (or more generally the UK) stems from volcanism in neighbouring regions of the UK such as Iceland. The annual probability of ash from a volcanic eruption exceeding a ground-level concentration of 5 µg/m^3 is estimated at about 1 in 300, with the duration of ash fall between 20 and 45 hours. The majority of ash particles are expected to be smaller than 10 micrometres (the respirable range), and the most likely source is a moderate-size Icelandic eruption. Higher ash concentrations have a 1-in-1000 annual probability. The confidence levels for these predictions are subject to assumptions regarding the frequency of suitable volcanic events and weather patterns, as well as the ability to model the movement of the ash; there remain some major uncertainties with respect to the prediction of volcanic events, particularly ash-producing moderate events.

The assessment of hazard combinations has looked at pairs of natural hazards. Natural hazards are often considered in isolation. However, it is possible for more than one natural hazard to occur simultaneously or for one hazard to occur soon after another and so enhance the impacts of an existing situation. This is particularly the case for severe weather events. Not all combinations of the thirty-two natural hazards noted for the ETI project were considered. Some combinations may be screened out because they are unphysical due to their nature. The inland location of the site means any maritime hazards can be ignored. Other combinations need some degree of assessment to identify those for which it is required or possible to carry out an in-depth characterisation. One realistic hazard combination, low summer rainfall

3. Conclusions

coinciding with high temperatures, was analysed in detail to provide an example of how to calculate the joint probability of a hazard combination. This illustrative calculation relied on the use of a copula to represent the dependence between low summer rainfall and high temperatures. The joint return period of mean summer maximum temperatures exceeding 22 °C and summer rainfall being below 100 mm at Trawsfynydd was calculated to be 115 years.

Further guidance on the characteristics and characterisation of these three families of natural hazards is provided in Volumes 2 — Extreme High and Low Air Temperature, 7 — Seismic, Volcanic and Geological Hazards and 12 — Hazard Combinations.

Case Study 1: Trawsfynydd

AghaKouchak A, Cheng L, Mazdiyasni O, Farahmand A. 2014. Global warming and changes in risk of concurrent climate extremes: Insights from the 2014 California drought. *Geophysical Research Letters,* 41, 8847–8852. *doi:10.1002/2014GL062308*

BBC. 2014. 'Ice pancakes' found floating on the River Dee. *http://www.bbc.co.uk/news/uk-scotland-north-east-orkney-shetland-30530281* (accessed on 26th March 2018).

BGS. 2018. UK historical earthquake database. *http://quakes.bgs.ac.uk/historical/query_eq/* (accessed on 26th March 2018).

Bommer J, Papaspiliou M, Price W. 2011. Earthquake response spectra for seismic design of nuclear power plants in the UK. *Nuclear Engineering and Design,* 241, 968–977. *doi: 10.1016/j.nucengdes.2011.01.029*

Brown I, Thompson D, Bardgett R, Berry P, Crute I, Morison J, Morecroft M, Pinnegar J, Reeder T, Topp K. 2016. *UK Climate Change Risk Assessment Evidence Report: Chapter 3, Natural Environment and Natural Assets.* London, UK. Available at: *https://www.theccc.org.uk/tackling-climate-change/preparing-for-climate-change/uk-climate-change-risk-assessment-2017* (accessed on 26th March 2018).

Burroughs L. (Ed.). 1998. Wave forecasting by manual methods. In *Guide to Wave Analysis and Forecasting,* WMO no. 702 (2nd edition). World Meteorological Organization, Geneva, Switzerland.

Chai T, Crawford A, Stunder B, Pavolonis MJ, Draxler R, Stein A. 2017. Improving volcanic ash predictions with the HYSPLIT dispersion model by assimilating MODIS satellite retrievals. *Atmospheric Chemistry and Physics,* 17, 2865–2879. *doi:10.5194/acp-17-2865-2017*

Clark MR. 2011. An observational study of the exceptional 'Ottery St Mary' thunderstorm of 30 October 2008. *Meteorological Applications,* 18, 137–154. *doi: 10.1002/met.187*

Coflein. 2018. Maentwrog dam, Trawsfynydd. *http://www.coflein.gov.uk/en/site/415006/details/maentwrog-dam-trawsfynydd* (accessed on 26th March 2018).

Coles S. 2001. *An Introduction to Statistical Modeling of Extreme Values.* Springer, London, UK.

Defra. 2005. *The threat posed by tsunami to the UK.* London. Available at: *http://www.onr.org.uk/fukushima/submissions/207061.pdf* (accessed on 26th March 2018).

Defra. 2010. *The River Basin Districts Typology, Standards and Groundwater Threshold Values (Water Framework Directive) (England and Wales) Directions 2010.* Available at: *http://archive.defra.gov.uk/environment/quality/water/wfd/documents/2010directions.pdf* (accessed on 26th March 2018).

Dupuis DJ. 2007. Using copulas in hydrology: benefits, cautions, and issues. *Journal of Hydrologic Engineering,* 12, 381–393. *doi:10.1061/(ASCE)1084-0699(2007)12:4(381)*

Ferro CAT, Segers J. 2003. Inference for clusters of extreme values. *Journal of the Royal Statistical Society: Series B (Statistical Methodology),* 65, 545–556. *doi:10.1111/1467-9868.00401*

Genest C, Boies J-C. 2003. Detecting dependence with Kendall plots. *The American Statistician, 57,* 275–284. *doi:10.1198/0003130032431*

Genest C, Remillard B, Beaudoin D. 2009. Goodness-of-fit tests for copulas: a review and a power study. *Insurance: Mathematics and Economics,* 44, 199–213. *doi: 10.1016/j.insmatheco.2007.10.005*

Giardini D, Woessner J, Danciu L, Crowley H, Cotton F, Grünthal G, Pinho R, Valensise L, and the SHARE consortium. 2013. *SHARE European Seismic Hazard Map for Peak Ground Acceleration, 10% Exceedance Probabilities in 50 Years.* *doi. 10.12686/SED-00000001-SHARE*

Gilleland E, Katz RW. 2016. extRemes 2.0: an extreme value analysis package in R. *Journal of Statistical Software, 72,* 1–39. *doi:10.18637/jss.v072.i08*

Goda K, Aspinall W, Taylor C. 2013. Seismic hazard analysis for the UK: sensitivity to spatial seismicity modelling and ground motion prediction equations. *Seismological Research Letters,* 84, 112–129. *doi: 10.1785/0220120064*

Heffernan JE, Tawn JA. 2004. A conditional approach for multivariate extreme values (with discussion). *Journal of the Royal Statistical Society: Series B (Statistical Methodology),* 66, 497–546. *doi: 10.1111/j.1467-9868.2004.02050.x*

HM Government. 2010. *The Air Quality Standards Regulations 2010.* *http://www.legislation.gov.uk/uksi/2010/1001/contents/made* (accessed on 26th March 2018).

IPCC. 2013. Summary for policymakers. In *Climate Change 2013: The Physical Science Basis. Contribution of Working Group I to the Fifth Assessment Report of the Intergovernmental Panel on Climate Change* (pp. 1–30). Cambridge University Press, Cambridge, UK and New York, NY.

Jamieson A. 2010. Britain's big freeze in pictures: Derwentwater in Lake District turns to ice. *http://www.telegraph.co.uk/news/weather/6956420/Britains-big-freeze-in-pictures-Derwentwater-in-Lake-District-turns-to-ice.html* (accessed on 26th March 2018).

Jenkins GJ, Perry MC, Prior MJ. 2008. *The climate of the UK and recent trends.* Available at: *http://ukclimateprojections.metoffice.gov.uk/media.jsp?mediaid=87933&filetype=pdf* (accessed on 26th March 2018).

Jenkins SF, Wilson TM, Magill CR, Stewart C, Marzocchi W, Boulton M. 2015. *Volcanic ash fall hazard and risk: technical background paper.* Available at: *http://www.preventionweb.net/english/hyogo/gar* (accessed on 26th March 2018).

Ledford AW, Tawn JA. 1997. Modelling dependence within joint tail regions. *Journal of the Royal Statistical Society: Series B (Statistical Methodology),* 59, 475–499. *doi:10.1111/1467-9868.00080*

Loughlin SC, Sparks S, Brown SK, Jenkins SF, Vye-Brown C. (Eds.). 2015. *Global Volcanic Hazards and Risk.* Cambridge University Press, Cambridge, UK.

Case Study 1: Trawsfynydd

Magnox. 2018. Trawsfynydd. *magnoxsites.com/site/trawsfynydd* (accessed on 26th March 2018).

Meaden GT. 1982. Hailstorms in north-east Bristol, 18th June 1982, and Ludlow, 26th June 1982. *Journal of Meteorology, 7*, 224–225.

Met Office. 2011. Winter 2010/11.
http://www.metoffice.gov.uk/climate/uk/summaries/2011/winter
(accessed on 26th March 2018).

Met Office. 2016. Storm Frank.
https://www.metoffice.gov.uk/barometer/uk-storm-centre/storm-frank
(accessed on 26th March 2018).

Met Office. 2017a. Storm Brian.
https://www.metoffice.gov.uk/barometer/uk-storm-centre/storm-brian
(accessed on 26th March 2018).

Met Office. 2017b. Why does it rain?
https://www.metoffice.gov.uk/learning/rain/why-does-it-rain
(accessed on 26th March 2018).

Murphy JM, Sexton DMH, Jenkins GJ, Boorman PM, Booth BBB, Brown CC, Clark RT, Collins M, Harris GR, Kendon EJ, Betts RA, Brown SJ, Howard TP, Humphrey KA, McCarthy M, McDonald RE, Stephens A, Wallace C, Warren R, Wilby R, Wood RA. 2009. *UK Climate Projections Science Report: Climate change projections.* Met Office Hadley Centre, Exeter, UK. Available at: *http://ukclimateprojections.defra.gov.uk* (accessed on 26th March 2018).

Musson RMW, Sargeant SL. 2007. *Eurocode 8 seismic hazard zoning maps for the UK* (Technical report CR/07/125). British Geological Survey, Nottingham, UK. Available at: *http://www.earthquakes.bgs.ac.uk/hazard/UK_seismic_hazard_report.pdf* (accessed on 26th March 2018).

Perry M, Hollis D. 2005. The development of a new set of long-term climate averages for the UK. *International Journal of Climatology,* 25, 1023–1039. *doi:10.1002/joc.1160*

Perry M, Hollis D, Elms M. 2009. *The Generation of Daily Gridded Datasets for Temperature and Rainfall for the UK.* National Climate Information Centre, Met Office, Exeter, UK.

Prior J, Beswick M. 2008. The exceptional rainfall of 20 July 2007.
Weather, 63, 261–267. *doi:10.1002/wea.308*

R Core Team. 2013. *R: a language and environment for statistical computing.*
R Foundation for Statistical Computing, Vienna, Austria. *http://www.r-project.org/*
(accessed on 26th March 2018).

Requena AI, Mediero L, Garrote L. 2013. A bivariate return period based on copulas for hydrologic dam design: accounting for reservoir routing in risk estimation. *Hydrology and Earth System Sciences,* 17, 3023–3038. *doi: 10.5194/hess-17-3023-2013*

Roach WT, Brownscombe JL. 1984. Possible causes of the extreme cold during winter 1981–82. *Weather,* 39, 362–372. *doi: 10.1002/j.1477-8696.1984.tb06746.x*

Sanderson MG, Economou T, Salmon KH, Jones SEO. 2017. Historical trends and variability in heat waves in the United Kingdom. *Atmosphere,* 8, 191. *doi: 10.3390/atmos8100191*

Sanderson MG, Ford GP. 2016. Projections of severe heat waves in the United Kingdom. *Climate Research,* 71, 63–73. *doi: 10.3354/cr01428*

Schaefer VJ. 1950. The formation of frazil and anchor ice in cold water. *Eos, Transactions, American Geophysical Union,* 31, 885–893. *doi: 10.1029/TR031i006p00885*

Silverman BW. 1986. *Density Estimation for Statistics and Data Analysis.* Chapman & Hall, New York, USA.

The Guardian. 2003. France faces nuclear power crisis.
https://www.theguardian.com/news/2003/aug/13/france.internationalnews
(accessed on 26th March 2018).

UNEP. 2004. *Impacts of summer 2003 heat wave in Europe* (Environment Alert Bulletin).
Available at: *https://www.unisdr.org/files/1145_ewheatwave.en.pdf*
(accessed on 26th March 2018).

Case Study 1: Trawsfynydd

University of Bristol. 2016. *Volcanic Ash Hazard Assessment for UK Nuclear Sites.*

Welsh Government. 2017. *Grassland fires, 2016–17.*
http://gov.wales/docs/statistics/2017/171018-grassland-fires-2016-17-en.pdf
(accessed on 26th March 2018).

Welsh Government. 2018. *Grassland fires statistics.*
http://gov.wales/statistics-and-research/grassland-fires
(accessed on 26th March 2018).

Whitehouse JW. 1971. Some aspects of the biology of Lake Trawsfynydd; a power station cooling pond. *Hydrobiologia,* 38, 253–288. *doi: 10.1007/BF00036839*

Woolway RI, Carrea L, Merchant CJ, Dokulil M, de Eyto E, DeGasperi C, Korhonen J, Marszelewski W, May L, Paterson A, Rimmer A, Rusak J, Schladow G, Schmid M, Shimaraeva S, Silow E, Timofeev M, Verburg P, Watanabe S, Weyhenmeyer G. 2017. Lake surface temperature [in "State of the Climate in 2016"]. *Bulletin of the American Meteorological Society,* 98, 13–14. *doi: 10.1175/2017BAMSStateoftheClimate.1*

Zidikheri MJ, Lucas C, Potts RJ. 2017. Estimation of optimal dispersion model source parameters using satellite detections of volcanic ash. *Journal of Geophysical Research: Atmospheres,* 122, 8207–8232. *doi: 10.1002/2017JD026676*

Akaike information criteria (AIC)

Provides an estimate of the quality of statistical models for a given set of data. If several models are fitted to the same data, AIC provides a measure of the quality of each model relative to the others. AIC therefore provides a method for model selection. It is important to note that AIC does not provide a test of a model in an absolute sense — i.e., whether the fit of the model to the data is poor or not.

Copula

A multivariate distribution function, which describes the dependence between two or more variables. Copulas are based on the theory that a joint distribution of two or more variables can be described in terms of the distribution of each variable (the marginal distribution functions; see below) and a copula that describes the dependence between the variables.

Cumulative distribution function (CDF)

The CDF of a random variable U, evaluated at some value u, is the probability that $U \leq u$. Hence, the CDF has values between 0 and 1.

Geometrical Epicentral Cell

A method employed to develop seismic hazard maps.

Kendall's tau

A rank correlation coefficient, which provides a measure of the statistical dependence of two datasets. It has values between −1 and 1. A value close to 1 would indicate the values in the two datasets have similar or identical ranks. Values near 0 indicate little or no correlation between the datasets.

Kernel smoothing

A statistical technique to estimate a real valued function as the weighted average of neighbouring observed data.

Marginal distribution function

Gives the probability of values of a random variable within a larger dataset without reference to the other variables.

North Atlantic Oscillation (NAO)

A large-scale pressure pattern that has important impacts on the weather and climate of the North Atlantic region and Europe. Its influence is strongest during winter, but can also affect summer weather. High latitudes, near Greenland and Iceland, generally experience low air pressures, whilst air pressures further south (near the Azores) are higher. The exact air pressure, and positions of the centres of the low and high pressure regions, vary over time. The NAO reflects fluctuations in the difference in pressure between these two regions. If the air pressure is lower than average over Iceland and higher than average over the Azores, the NAO is in a positive phase, which corresponds to stormy conditions and mild and wet winters over northern Europe. If the air pressures over Iceland and the Azores are higher and lower than average respectively, the NAO is in a negative phase. A negative NAO corresponds to decreased storminess, below-average precipitation, and cold temperatures over northern Europe during winter.

Shear wave

A type of elastic wave, which propagates through the body of an object, unlike surface waves.

AEP	Annual exceedance probability
AIC	Akaike information criteria
BBC	British Broadcasting Company
BGS	British Geological Survey
CAA	Civil Aviation Authority
CDF	Cumulative distribution function
Defra	Department for Environment, Food and Rural Affairs
ETI	Energy Technologies Institute
EUR	European Utility Requirements
EVA	Extreme value analysis
GEV	Generalised extreme value
HVAC	Heating, ventilation, and air conditioning
ICAO	International Civil Aviation Organization
IPCC	Intergovernmental Panel on Climate Change
NAO	North Atlantic Oscillation
NATS	National Air Traffic Services
NERC	Natural Environment Research Council
PGA	Peak ground acceleration
PP-GPD	Poisson generalised Pareto distribution
SHARE	Seismic hazard harmonisation in Europe
UNEP	United Nations Environment Programme
VAAC	Volcanic Ash Advisory Centre
VAA	Volcanic Ash Advisory
VAG	Volcanic Ash Graphic